

Supplementary Data and Discussion

Recombinant IL-35. In our hands, recombinant IL-35 has proven to be a poorly produced and relatively unstable cytokine. Thus far, our studies suggest that the HEK293T, CHO, COS, Baculovirus, Drosophila S2, *Pichia pastoris* and *E.coli* expression systems are unable to secrete the appreciable quantities of recombinant mouse or human IL35 required for purification. While we cannot rule out the possibility that a unique fusion protein or modification may yield significantly improved production, it seems likely that it will not be possible to produce significant quantities of native IL-35 in any currently known expression system.

Human IL-35 validation. We used three approaches to verify that the recombinant IL35 generated by 293T, and no other suppressive factor, mediates conversion of T_{conv} to a suppressive population. First, IL-35 was removed from IL-35 supernatants using anti-p35 antibody coupled Protein G beads. Removal of IL-35 by immunoprecipitation completely abolished the ability of the IL-35 supernatants to suppress T_{conv} cell proliferation, suggesting that all the suppressive activity is due to IL-35, and no other factors present in the supernatants (Supplementary Fig. 2). Second, T cells were treated with IL-35 alone or in the presence of IL-10, TGF β or IL-35 neutralizing (clone 27537) (R&D Systems) antibodies. While neutralization of IL-10 and TGF β had no effect on the ability of cells to acquire suppressive capacity, neutralization of IL-35 almost completely inhibited conversion (Fig. 1g and Supplementary Fig. 2). Control protein was unable to induce conversion or suppressive capacity regardless of whether any of the neutralizing antibodies were included in the assays (data not shown). Third, IL-35 was coupled to Protein G beads via neutralizing (clone 27537) (R&D Systems) or non-neutralizing (clone 45806) (R&D Systems) anti-p35 mAbs. Importantly, the ability of the two antibodies to immunoprecipitate IL-35 is equivalent (data not shown). In addition, these anti-p35 mAbs appear to be IL-35 specific as they have no effect on IL-12 activity (data not shown). Following conjugation with IL-35, beads were washed and subsequently used for suppression

assays, in the absence of any supernatant. Beads coupled with IL-35 via non-neutralizing, but not neutralizing anti-p35 mAbs, suppressed the proliferation of T_{conv} cells in a titratable fashion (Supplementary Fig. 2). Control protein-coupled beads had no effect on the proliferation of T_{conv} cells. Taken together, these data demonstrate beyond a reasonable doubt that 293T-generated IL-35 alone mediates the bioactivity observed.

Human IL-35 is suppressive and IL-35-treated T_{conv} acquire a regulatory phenotype.

Human umbilical cord blood is an ideal source of naive T_{conv} and nT_{regs} due to their lack of previous antigenic exposure, and thus the ease with which they can be reliably purified based on CD4 and CD25 expression (Supplementary Fig. 1). Purified cord blood T_{regs} exhibit uniform Foxp3 expression, while T_{conv} lack Foxp3 expression, demonstrating purity. As previously shown with murine IL-35, human IL-35 can suppress the proliferation of human T_{conv} cells in a dose-dependent manner (Supplementary Fig. 2). The degree of suppression by IL-35 is similar to that seen by activated T_{regs} .

Murine IL-35 validation. Similar validation experiments were performed with murine IL-35 as described for human IL-35 above. First, removal of IL-35 by immunoprecipitation completely abolished the ability of the IL-35 supernatants to suppress T_{conv} cell proliferation, suggesting that all suppressive activity is due to IL-35 and no other factors present in the supernatants (Supplementary Fig. 4). Second, addition of neutralizing murine IL-35 mAb [V1.4H6.25], but not non-neutralizing [clone 25806] abrogates the ability of murine IL-35 containing 293T-generated supernatant to mediate IL-35 iT_R conversion (Supplementary Fig. 4). In addition, quantification of rIL-35 in 293T-generated supernatants was determined using an IL-35-specific ELISA. Our results suggest that the 293T cells generate approximately 5-10ng/ml recombinant IL-35 (Supplementary Fig. 4). Additional calculations to account for dilution and dialysis into media appropriate for functional assays indicate that generating iT_{R35} using our standard conversion protocol (whereby 25% of the total culture volume is 293T-generated IL-35) requires

approximately 500-700pg/ml rIL-35.

IL-35 treated murine T_{conv} acquire a regulatory phenotype *in vitro*. The induction of *Ebi3* and *Il12a* expression was unique to IL-35 treated cells when compared to untreated, rIL-10, rIL-27 or rTGF β treated cells (Supplementary Fig. 5). Following a 3 day treatment with IL-35, cells express *Ebi3* and *Il12a* but not *Il12b*, *Il27a* or *Il23a*, ruling out any role for IL12, IL23 or IL27 in the suppressive activity of these cells (Supplementary Fig. 5).

No role for TGF β in IL-35 iT_R conversion or function. To determine the role of TGF β in conversion, we utilized cells that were unable to respond to TGF β [*TGF β R.DN* –mice expressing a dominant negative mutant of the TGF β receptor ¹] for conversion or as responder cells. Our results indicate that TGF β does not mediate the generation of this iT_R population nor mediates their regulatory activity, consistent with their lack of TGF β expression (Supplementary Fig. 5 and 7).

Affymetrix GeneChip microarray analysis of IL-35- and control-treated T_{conv} cells. IL-35-treated T_{conv} cells expressed *Ebi3* and *Il12a* mRNA, as determined by qPCR analysis, secrete IL-35, as determined by IP/western blot, and suppress T_{conv} in suppression assays (Supplementary Fig. 10). However, *Ebi3* and *Il12a* were not reliably detected by Affymetrix GeneChip microarray analysis (Supplementary Fig. 10 and 11). However, not all probe sets on these arrays work effectively and it is thought that cytokine genes are not effectively detected by Affymetrix GeneChip microarrays. Thus, we cannot preclude the possibility that other molecules with poor probe sets may identify iT_R35 but were not identified by Affymetrix analyses. Similar to previously published analyses², we performed a meta-analysis that compared gene expression profiles of T_{reg} cells to T_{conv} in an effort to define a T_{reg} genetic signature. We then aimed to determine whether IL-35 treated T cells, which acquired suppressive capacity, would also acquire components of the T_{reg} genetic signature. Five IL-35 treated samples, in parallel with control-treated samples, were compared to T_{reg} and T_{conv} cells.

Expression of each of the T_{reg} signature genes was scaled from 0 to 1, where a score of 0 was blue 0.5 was black and 1 was yellow, and the gene scores graphically represented as a heat map. Our results indicate that both control and IL-35 treated T_{conv} share some expression patterns with both T_{reg} and T_{conv} cells. However, their expression patterns were nearly identical to one another, suggesting that modest transcriptional changes are responsible for the phenotype observed in IL-35 treated cells.

TGF β is not required for *in vivo* suppression by iT_{R35} . We used the recovery model of IBD to further assess the involvement of TGF β in iT_{R35} function. Purified wild-type or *TGF β R.DN* naïve T cells were adoptively transferred into *Rag1^{-/-}* hosts. Following clinical signs of sickness, mice were treated with iT_{R35} cells to initiate recovery from IBD. Mice receiving either wild-type T_{conv} cells or cells that were unable to respond to TGF β (*TGF β R.DN*) developed IBD to a similar degree, as determined by weight loss and histological analysis (Supplementary Fig. 14). In addition, iT_{R35} cells were equally capable of curing IBD caused by wild type and *TGF β R.DN* (Supplementary Fig. 14). This suggests that TGF β is not required for suppression by iT_{R35} *in vivo*.

T_{reg} -mediated suppression generates iT_{R35} . To determine whether n T_{reg} or suppressed T_{conv} -derived IL-10 or IL-35 was required for the generation of the regulatory suppressed T_{conv} population, we assessed the proliferative and suppressive capacity of suppressed T_{conv} purified from n T_{reg} : T_{conv} co-cultures in which only one population was mutant. Interestingly, IL-35 from both cell types was required to induce conversion, as determined by the failure to acquire hyporesponsiveness and suppressive capacity (Fig. 5d-f). Real time PCR analysis demonstrated that the absence IL-35 production by the suppressed T_{conv} (due to the use of *Ebi3^{-/-}* or *Il12a^{-/-}* T_{conv}) significantly reduced expression of the non-targeted partner chain (eg. *Il12a* expression in *Ebi3^{-/-}* T_{conv}), implicating the presence of a positive autocrine loop in which the induction of IL-35 by suppressed T_{conv} is potentiated by its own production (Supplementary Fig. 17). However,

nT_{reg} -derived IL-35 is still required to initiate this process as $Ebi3^{-/-}$ nT_{regs} cannot mediate conversion. In contrast to the requirement for IL-35, nT_{reg} - but not suppressed T_{conv} -derived IL-10 was necessary to mediate conversion (Fig. 5d-f). This suggested that IL-10 may be required for the conversion mediated by nT_{regs} , but that once converted, suppressed T_{conv} may be capable of suppressing responder T_{conv} cell proliferation in the absence of IL-10. These data are consistent with the lack of IL-10 and TGF β expression in suppressed T_{conv} revealed by qPCR (Supplementary Fig. 16).

Previous studies and data presented here demonstrate that short-term exposure to IL-35 but not IL-10 can mediate iT_R conversion^{3,4}. Furthermore, IL-10 does not induce *Ebi3* and *Il12a* mRNA expression (Supplementary Fig. 5). We tested the possibility that IL-10 served to augment or potentiate the generation of iT_{R35} T_{conv} cells cultured with IL-35 and IL-10. As shown previously, IL-35, but not IL-10 treated cells, acquired suppressive capacity (Supplementary Fig. 16). However, at suboptimal concentrations of IL-35, exogenous IL-10 could potentiate conversion of iT_{R35} .

iT_{R35} contribute to the regulatory milieu *in vivo*. Following reconstitution, B16 melanoma cells were inoculated into mice, solid tumors resected 15-17 days post-transfer and T_{conv} and T_{regs} purified on the basis of congenic markers from spleens and tumors. As previously shown, both *Ebi3* and *Il12a* (p35) are expressed in T_{regs} , but not T_{conv} splenic T cells (Supplementary Fig. 17). Tumor infiltrating wild type T_{regs} and T_{conv} cells had significantly increased expression of both *Ebi3* and *Il12a*, as previously shown. Also noteworthy is the fact that unlike the wild-type $CD4^+Foxp3^-$ cells which upregulate both *Ebi3* and *Il12a* expression, $CD4^+Foxp3^-$ cells from $Ebi3^{-/-}$ mice fail to upregulate *Il12a* expression. This suggests coordinated expression of *Ebi3* and *Il12a*, the two components of IL-35.

Discussion. iT_{R35} cells represent a new member of the regulatory T cell family. iT_{R35} can be generated with a single, short term TCR stimulation in the presence of IL-35 (murine - 3 days;

human – 6 days) unlike other iT_R populations described previously, TGF β iT_R and IL-10 iT_R , which require longer conversion protocols, multiple cell types and/or additional molecules for optimal generation^{3, 5, 6}. iT_{R35} induction is independent of Foxp3 expression and does not require the other key suppressive cytokines, IL-10 or TGF β , for conversion (Supplementary Fig. 17). Single cell analysis of human iT_{R35} by intracellular cytokine staining and confocal microscopy suggests that IL-35, but not control protein, treatment induces homogeneous expression of IL-35 in human CD4⁺ T_{conv} cells (Fig. 1). Whether expression remains homogeneous in differing *in vivo* inflammatory situations, or with murine iT_{R35} remains to be determined. nT_{reg} -mediated suppression *in vitro* and perhaps *in vivo* may orchestrate the conversion of T_{conv} into iT_{R35} within the suppressed T_{conv} population, as evidenced by expression of IL-35, induction of hyporesponsiveness and acquisition of a regulatory phenotype (Fig. 5). These cells also acquire the Foxp3⁻/Ebi3⁺/Il12a⁺/Il10⁻/Tgfb⁻ iT_{R35} signature. The generation of iT_R cells within suppressed T_{conv} requires IL-35 and, to a lesser extent, IL-10. IL-10 may directly potentiate iT_{R35} generation by IL-35 producing T_{regs} or it may simply slow down T_{conv} activation and/or proliferation thus indirectly facilitating iT_{R35} conversion. Importantly, iT_{R35} are potently suppressive in a variety of *in vitro* and *in vivo* models. In addition, our studies with B16 melanoma suggest that iT_{R35} can be generated *in vivo* and may be stable, although this will require further study.

Supplementary Methods

Mice. $Ebi3^{-/-}$ mice (C57BL/6: now 100% C57BL/6 by microsatellite analysis performed by Charles River) were initially provided by R. Blumberg and T. Kuo. $Foxp3^{gfp}$ mice (C57BL/6: now 100% C57BL/6 by microsatellite analysis) were provided by A. Rudensky and V. Kuchroo. $Foxp3^{-/-}$ were provided by J. Ihle with permission from A. Rudensky. $Il10^{-/-}$ mice were provided by T. Geiger. TGF β R.DN, $Il12a^{-/-}$, $Rag1^{-/-}$, C57BL/6 and B6.PL mice were purchased from the Jackson Laboratory. All animal experiments were performed in American Association for the Accreditation of Laboratory Animal Care-accredited, specific-pathogen-free facilities in the St. Jude Animal Resource Center following national, state and institutional guidelines. Animal protocols were approved by the St. Jude Animal Care and Use Committee. *Trichuris muris* infection experiments were performed at a specific pathogen-free facility at the University of Pennsylvania under Institutional Animal Care and Use Committee (IACUC) approved protocols and in accordance with the guidelines of the IACUC of the University of Pennsylvania.

Human umbilical cord blood and peripheral blood. Human UCB was obtained from the umbilical vein immediately after vaginal delivery with the informed consent of the mother and approved by St. Louis Cord Blood Bank Institutional Review Board. Human peripheral blood mononuclear cells were obtained from apheresis rings obtained from the St. Jude Blood Donor Center. All use at St. Jude was approved by the St. Jude IRB.

IL-35 mAbs. Recombinant murine Ebi3 was cloned and expressed in a proprietary *E. coli* expression system by Mike Jones (Shenandoah Biotechnology). *E. coli* were fermented and inclusion bodies produced and refolded. Properly folded protein was purified by size exclusion and ion exchange, quantitated, sterile filtered through a 0.2 micron filter and lyophilized. Six week old $Ebi3^{-/-}$ mice were given intraperitoneal injections on week zero, three and seven with 50 μ g of recombinant Ebi3 protein in complete Freund's. Following an initial screen, the mice with the highest anti-Ebi3 serum titers were hyperimmunized intravenous 3 days and 2 days

prior to fusion with 40 μ g recombinant Ebi3 protein in PBS. The spleens were fused with X63-Ag8.653 myeloma cells and the clones screened by ELISA for anti-Ebi3 activity using a direct ELISA with recombinant Ebi3 protein absorbed to an ELISA plate (Jackson Immuno Research, West Grove, PA) and anti-Ebi3 activity detected with a goat anti-mouse HRP (Fisher, Hanover Park, IL). Positive clones were subcloned and re-screened. Supernatant from clones V1.4F5.29, V1.4H6.25, and V1.4C4.22 were purified over protein G Sepharose (GE Healthcare, Piscataway, NJ). These clones were subsequently screened for cross reactivity to human IL-35, as well as their capacity to IP, blot, and neutralize bioactivity. Clone V1.4H5.29 cross-reacts with human EBI3 and was used for probing Western blots. Clone V1.4H6.25 was used in *in vitro* mIL-35 neutralizing studies and clone V1.4C4.22 was used in *in vivo* mIL-35 neutralizing studies. Both the p35 and Ebi3 antibodies used are capable of recognizing IL-12 and IL-27, respectively, by IP however neutralization was IL-35 specific as demonstrated in IL-12 (data not shown) and IL-27 bioassays (Supplementary Fig. 8). The following additional antibodies were also used: anti-p35 for immunoprecipitation of murine (clone 45806) (R&D Systems) and human IL-35 (clone 27537) (R&D Systems). In addition, clone 27537 (R&D Systems) was found to neutralize hIL-35 bioactivity while clone 45806 (R&D Systems) was used as a non-neutralizing m/h IL-35 mAb control. The Ebi3 antibody, clone 355028 (R&D systems), was used for ELISA capture.

IL-27 Bioassay. Purified murine T_{conv} cells were activated with anti-CD3 and anti-CD28 mAb (10 μ g/ml) in the presence of rIL-27 and rIL-12 (50ng/ml) and neutralizing anti-IL-2 mAb for 4 days. IL-27 activity was measured by determining IFN γ secretion in the presence of anti-IL-35 mAbs V1.4C4.22 and V1.4F5.25 or neutralizing anti-Ebi3 mAb AF1834 or isotype control (R&D Systems), at a final concentration of 10 μ g/ml.

mIL-35 ELISA. Anti-mouse Ebi3 (clone 355028 - 2 μ g/ml) (R&D systems) mAb was coated on 96-well, flat-bottom microtiter plates (Dynatech Laboratories, Franklin, MA) in PBS overnight at

room temperature. The plates were washed three times with PBS-Tween 20 (0.05%) and then blocked with PBS+ 1% BSA for 2h at room temperature. The plates were washed, and standard or 293T cell culture medium was added. After 2h incubation at room temperature, the plates were washed, then probed with 1 μ g/ml biotinylated rat anti-mouse p35 (clone 45806) (R&D Systems), diluted in PBS + 1% BSA. The plate was incubated at room temperature for an additional 2h. This was followed by three washes and a 20 minute incubation with streptavidin-HRP secondary Ab (1/2000 dilution in PBS + 1% BSA; Amersham Biosciences). Plates were developed with tetramethylbenzidine substrate solution (Pierce) in the dark, for 20 minutes at room temperature, and the reaction was stopped by adding 50 μ l of 1 N H₂SO₄ to each well. Absorbance was measured with a spectrophotometer at A450 (Molecular Devices, Sunnyvale, CA). The IL-35 concentration was calculated using a purified murine IL-35:Fc (mIL-35-Fc) fusion protein generated in NSO cells.

Transfection of HEK293T cells for IL-35 and control protein generation. IL-35 constructs were generated by recombinant PCR as described⁷, and cloned into pPIGneo, a pCIneo-based vector (Promega) that we have modified to include an IRES-GFP cassette. A construct containing Ebi3 and Il12a linked by a flexible glycine-serine linker was used for IL-35 generation and an empty pPIGneo vector was used as a control. HEK293T cells were transfected using 10 mg plasmid per 2x 10⁶ cells using TransIT transfection reagent (Mirus). Cells were sorted for equivalent GFP expression and were cultured for 36 h to facilitate protein secretion. Dialyzed, filtered supernatant from cells was used at 25% of total culture medium to induce conversion of T_{conv} cells into iT_R35.

Anti-CD3/CD28-coated latex beads. 4 μ M sulfate latex beads (Molecular Probes) were incubated overnight at room temperature with rotation in a 1:4 dilution of anti-CD3 + anti-CD28 antibody mix (13.3 μ g/ml anti-CD3 (murine clone # 145-2c11, human clone # OKT3) (eBioscience) and 26.6 μ g/ml anti-CD28 (murine clone # 37.51, human clone # CD28.6)

(eBioscience). Beads were washed 3 times with 5mM phosphate buffer pH 6.5 and resuspended at 5×10^7 /ml in sterile phosphate buffer with 2mM BSA.

Recombinant IL-35 validation experiments. Beads were generated that presented IL-35 in a suppressive or non-suppressive format. Neutralizing (for non-suppressive beads - 1 μ g clone 27537) (R&D Systems), non-neutralizing (for suppressive beads - 1 μ g clone 25806) or appropriate isotype controls (human IgG1 or rat IgG2) mAbs were added to 1ml of IL-35 supernatant or control supernatant and rotated at 4°C for 4h. Protein G beads were added and rotated for an additional 12-18 h. To ensure the protein was attached to the beads, the beads were boiled to release bound protein, resolved by SDS-PAGE and probed with anti-Ebi3 mAb. Both the beads and post IP supernatant were tested for functional activity in a standard suppression assay. To determine suppressive capacity, the panel of conjugated beads were washed thoroughly in PBS and resuspended in culture media prior to assay. Beads or post IP supernatant were added cultured with T_{conv} in medium containing anti-CD3 + anti-CD28 conjugated beads as indicated for 6 days. Anti-CD3 + anti-CD28 beads were used at a ratio of 1:1 (cell:bead), whereas the IL-35 beads were titrated in a dose dependent manner. Unconjugated IL-35 supernatant was used as a control. Proliferation was determined by [3 H]-thymidine incorporation.

Flow cytometric analysis, intracellular staining and cell sorting. T_{conv} ($CD4^+CD25^-CD45RB^{hi}$) and T_{reg} ($CD4^+CD25^+CD45RB^{lo}$) cells from the spleens and lymph nodes of C57BL/6 or knockout age-matched mice were positively sorted by FACS. After red blood cell lysis, cells were stained with antibodies against CD4, CD25 and CD45RB (Biolegend) and sorted on a MoFlo (Dako) or Reflection (i-Cyt). Cell surface molecules including CD4, CD69, CD25, CD73 (Biolegend), LA G-3, CTLA-4 and CD28 (BD Pharmingen) were stained with fluorescently conjugated mAbs. Flow cytometric analysis was performed as detailed previously⁷, using a FACSCalibur (Becton Dickinson). For intracellular staining, human cord T_{conv} , were isolated by

FACS and activated for 9 days with anti-CD3- + anti-CD28-coated latex beads (see generation below) in the presence of control or IL-35 supernatant as 25% of culture media⁸. The cells were purified 9 days later and analyzed for the expression of p35. A cell were used for the intracellular staining. For analysis of intracellular IL-35 production, purified T cells (0.5×10^6 minimum) were first activated with PMA (10nM) + ionomycin (10nM) for 5h with brefeldin (1:100) (BD Bioscience) added for the final 4h of activation. Cells were surface stained with anti-CD4-Alexa 647 (Biolegend) prior to intracellular staining. Fixation and permeabilization was performed using a proprietary permeabilization buffer, referred to as 8E, a paraformaldehyde-based reagent developed in the laboratory of Dario Campana (St Jude Children's Research Hospital). The cells were then stained for intracellular IL-35 with anti-p35-PE (clone 27537) (R&D Systems) or IgG1 isotype control-PE (R&D Systems clone #11711) for 30 minutes at 4°C and analyzed by flow cytometry. Samples were analyzed on a FACSCalibur using Cell Quest software (BD Biosciences). FlowJo 5.7.0 software was used for data analysis.

Murine iT_{R35} , suppressed T_{conv} , suppressive T_{reg} and $TGF\beta$ iT_R . Purified murine T_{conv} cells from wild-type C57BL/6, $Ebi3^{-/-}$ and $Foxp3^{-/-}$ were activated by anti-CD3- + anti-CD28-coated latex beads in the presence of various cytokines to for iT_R conversion protocols. Culture medium from control or IL-35 transfected 293T cells (dialyzed against media and filtered) was added to cultures at 25% of total culture volume as the source of control or IL-35 protein in the generation of murine iT_{R35} ⁸. Where indicated, recombinant IL-10, $TGF\beta$, or IL-27 was added at 100ng/ml to compare cytokine activity of IL-10, $TGF\beta$, or IL-27 to IL-35. Cells were cultured for 72 hours and re-sorted for proliferation, suppression or *in vivo* functional assays of iT_{R35} activity. To generate suppressed T_{conv} , and suppressive T_{reg} , purified T_{conv} cells were activated in the presence of anti-CD3- + anti-CD28-coated latex beads and wild-type or knockout T_{regs} (as indicated) for 72 hours. Suppressed T_{conv} and suppressive T_{regs} from the co-culture were re-sorted on the basis of congenic markers or CFSE labeling and used for phenotyping,

proliferation, suppression or *in vivo* functional assays of activity. For TGF β iT_R cell conversion, 5ng/ml TGF β was added to cultures containing T_{conv} and anti-CD3- + anti-CD28-coated beads and cells were incubated for 5 days prior to analysis. In indicated assays, 100ng/ml neutralizing anti-IL-10 antibody (clone JES5-2A5, BD Bioscience) or neutralizing TGF β (Invitrogen) were added to during conversion or subsequent suppression assays.

Human IL-35 suppression and iT_R35 conversion. Human umbilical cord samples were provided by Brandon Triplett, Donna Regan, Michelle Howard and Melissa McKenna at the St. Louis Cord Blood Bank. Human peripheral blood was obtained from apheresis rings obtained from the St. Jude Blood Donor Center. Mononuclear cells were separated on Ficoll gradient and T_{conv} and T_{reg} cells were purified by FACS on the basis of anti-CD4 and anti-CD25 expression (Biolegend). Anti-CD45RA was added as an additional marker to purify T_{conv} and T_{reg} from peripheral blood. Purity of purified populations was verified using an intracellular Foxp3 staining kit (eBioscience). T_{conv} cells were cultured in X-vivo medium supplemented with 20% human sera (Lonza) and 100units/ml human IL-2 and activated by anti-hCD3- + anti-hCD28-coated latex beads (bead conjugation described above). Human IL-35 was generated as described for murine IL-35⁸. Suppression of T_{conv} cell proliferation by IL-35, control supernatant, or activated T_{regs} was determined by titrating suppressive factor into the culture. Culture medium from control or IL-35 transfected 293T cells (dialysed against media and filtered) was added to cultures at 25% of total culture volume as the source of control or IL-35 protein in the generation of human iT_R35. Cells were cultured for 9 days and re-sorted for proliferation and suppression assays to assess iT_R35 activity. To assess iT_R35 activity, iT_R35 cells were cultured with their own human T_{conv} cells at a ratio of 4:1 (T_{conv}:suppressor). T_{conv} cells were activated in the presence of anti-hCD3- + anti-hCD28-coated latex (as indicated) for 6 days, and the ability of human T_{conv} to proliferate in presence of iT_R35 was assessed by [³H]-incorporation for the final 8h of the incubation period.

For use in suppression assays with iT_{R35} , T_{conv} cells were stored frozen and thawed prior to use. For freezing, purified T_{conv} were washed three times in X-vivo medium with no additives. The pellet was resuspended in 0.5ml medium containing 10% DMSO and 20% human sera. The cells were immediately transferred to nalgene freezing box containing ethanol and stored in -80°C for minimum of 4h but no longer than 12h. Cells were then immediately transferred to liquid nitrogen and remained there until use in suppression assays. T_{conv} were removed from liquid nitrogen immediately thawed at 37°C . The cells were then transferred to 10ml conical tube and media added drop wise, while mixing the cells gently. The cells were washed three times, and viability was determined by trypan blue dye exclusion prior to use in suppression assays.

Confocal microscopy. $iT_{Rcontrol}$ and iT_{R35} were generated from human T_{conv} sorted from cord blood as described above. Purified cells were plated onto a Poly-L-lysine-coated chambered coverglass (Nunc) and cultured for 4 h at 37°C . Following incubation, cells were fixed with 4% methanol-free formaldehyde (Polysciences Inc) for 15 min at room temperature, followed by permeabilization in PBS containing 0.2% Triton-X-100. Cells were subsequently washed 3 times prior to incubation for 1 h in PBS containing 3% BSA and 5% normal goat serum. Following incubation in blocking solution, cells were stained overnight at 4°C with anti-human IL12A (p35) or isotype control antibodies (R&D Systems) directly conjugated to phycoerythrin. The actin cytoskeleton was detected with Alexa 488-conjugated phalloidin (Molecular Probes) and nuclei were labeled using DAPI (Molecular Probes). Cells were washed with PBS, and imaged using a Zeiss inverted spinning disc confocal microscope and Slidebook acquisition and analysis software (Intelligent Imaging Innovations).

Cytokine analysis. Murine $iT_{Rcontrol}$ and iT_{R35} were generated as described above. Purified cells were cultured for 72 h in the presence of anti-CD3- + anti-CD28-coated latex beads. Cell culture supernatants were harvested and analyzed for secretion of soluble factors. A Multi-plex Milliplex bead based analysis (Millipore) was used to simultaneously quantitate secretion of 26

different cytokines/chemokines.

RNA, cDNA and quantitative real-time PCR. Purified T_{conv} from C57BL/6 or age-matched knockout mice were treated as indicated. RNA was isolated using the Qiagen microRNA extraction kit following the manufacturer's instructions. RNA was quantified spectrophotometrically, and cDNA was reverse-transcribed using the cDNA archival kit (Applied Biosystems) following the manufacturer's guidelines. TaqMan primers and probes were designed with PrimerExpress software and were synthesized in the St Jude Hartwell Center for Biotechnology and Bioinformatics. The cDNA samples were subjected to 40 cycles of amplification in an ABI Prism 7900 Sequence Detection System instrument according to the manufacturer's protocol. Quantification of relative mRNA expression was determined by the comparative C_T (critical threshold) method as described in the ABI User Bulletin number 2 (<http://docs.appliedbiosystems.com/pebi/docs/04303859.pdf>), whereby the amount of target mRNA, normalized to endogenous β -actin, β -glucuronidase or cyclophilin expression, is determined by the formula $2^{-\Delta\Delta C_T}$.

Immunoprecipitation and Western Blotting Immunoprecipitation and immunoblotting were performed as previously described^{33,34}. T_{conv} , T_{reg} and suppressed T_{conv} were purified from spleens or tumors of mice, as indicated. iT_{Rcon} and iT_{R35} were generated as described above. All cells were cultured for 24 h and culture supernatants collected for analysis. To all supernatants, lysis buffer containing 0.1% Tween 20, 50 mM HEPES, 150 mM NaCl, 1 mM EDTA, 2.5 mM EGTA, and 1 complete protease inhibitor tablet (Roche, Indianapolis, IN) per 50 ml lysis buffer, was added. Supernatants were immunoprecipitated with anti-mouse II12a (p35-clone 45806) (R&D Systems) and Protein G-sepharose beads. Immunoprecipitates were resolved by SDS-PAGE (Invitrogen Life Technologies), and blots were probed with a biotinylated monoclonal anti-mouse Ebi3 antibody V1.4F5.29. Blots were developed using ECL (Amersham Biosciences) and autoradiography.

In vitro proliferation and suppression assays. To determine proliferative capacity of cells generated as described above, 2.5×10^4 cells were activated with anti-CD3- + anti-CD28-coated latex beads for 72 h. Cultures were pulsed with 1 mCi [3 H]-thymidine for the final 8 h of the 72 h assay, and were harvested with a Packard Micromate cell harvester. Counts per minute were determined using a Packard Matrix 96 direct counter (Packard Biosciences). Suppression assays were performed as described previously with some modifications⁹. Cytokine treated T_{conv} cells or suppressed T_{conv} suppressive capacity was measured by culturing 2.5×10^4 T_{conv} cells with anti-CD3- + anti-CD28-coated latex beads and 6.25×10^3 suppressor cells (see figures) (4:1 responder: suppressor ratio). Cultures were pulsed and harvested as described for proliferation assays. Transwell™ experiments were performed in 96-well plates with pore size $0.4 \mu\text{m}$ (Millipore, Billerica, MA). Freshly purified “responder” T_{conv} (5×10^4) were cultured in the bottom chamber of the 96-well plates in medium containing anti-CD3- + anti-CD28-coated latex beads. iT_{R35} or control treated T_{conv} in medium with anti-CD3- + anti-CD28-coated latex beads, were cultured in the top chamber. After 64 h in culture, top chambers were removed and [3 H]-thymidine was added directly to the responder T_{conv} cells in the bottom chambers of the original Transwell™ plate for the final 8 h of the 72 h assay. Cultures were harvested as described for proliferation and suppression assays

Affymetrix analysis of genetic signature. $iT_{Rcontrol}$ and iT_{R35} generation was verified by qPCR analysis of *Ebi3* and *Ii12a* expression as well as IL-35 secretion by immunoprecipitation and western blotting. RNA was extracted and quality was confirmed by UV spectrophotometry and by analysis on an Agilent 2100 Bioanalyzer (Agilent Technologies, Santa Clara, CA). Total RNA (100 ng) was processed in the Hartwell Center for Biotechnology & Bioinformatics according to the Affymetrix eukaryote two-cycle target labeling protocol. Biotin labeled cRNA (20 μg) was hybridized overnight at 45°C to the Mouse-430v2 GeneChip array, which interrogates more than 39,000 transcripts. After staining and washing, arrays were scanned and

expression values were summarized using the default parameters within MAS5 algorithm as implemented in the GCOS v1.4 software (Affymetrix, Santa Clara, CA). Signals were normalized for each array by scaling to a 2% trimmed mean of 500.

Nine T_{reg} samples, 3 of which were activated and 6 resting, were compared to 9 T_{conv} samples, 3 of which were activated and the remaining 6 resting. These samples were arrayed on Affymetrix U133 plus 2 arrays and MAS 5.0 signal data was collected and log-start transformed to stabilize the variance. T tests were applied to each probeset. Probesets that had a p value < 10e-5, an absolute value log ratio of T_{reg} versus T_{conv} of at least 3 (\log_2), and a defined gene name were selected. Next for each column in the signature plot the mean of that category was found. If a gene name appeared more than once then the mean data was averaged for that gene. The scores were calculated by finding the maximum and minimum values for each gene and then rescaling them from 0 to 1 by the following formula: $score_g = (\text{observed mean}_g - \text{minimum mean}_g) / (\text{maximum mean}_g - \text{minimum mean}_g)$ for each gene g . These gene scores were then sorted in descending order by the $T_{reg} : T_{conv}$ log ratio that includes activated and resting cells and graphed as a Heat map in Spotfire DecisionSite. A score of 0 is blue 0.5 is black and 1 is yellow, intermediate values are shaded on this scale. Magnitude and abundance plots (MA) and volcano plots were generated using S TATA/SE 11.0 (College Station, TX). Statistical tests and batch effect removal was performed using Partek Genomics Suite (St Louis, MO). The expression data from the Affymetrix U133 plus 2 arrays was analyzed as MAS 5.0 signal log-start transformed using the following formula: $\log \text{ signal} = \ln(\text{signal} + 20)$. This transform improves data dispersion, normality and stabilizes the variance of the data¹⁰. The small additive factor 20 is approximately the standard deviation of the background and is sufficient to prevent extreme ratios due to small signal differences at the low end of expression. The \log_2 ratios are calculated in STATA by the following formula: $\log \text{ratio A over B} = \log(\exp(\text{mean log signal A}) / \exp(\text{mean log signal B})) / \log(2)$. Average log signal in the MA plots

is simply the average of the two means in the logratio: $A = (\text{mean log signal A}) + (\text{mean log signal b})/2$. The T_{reg} and T_{conv} comparison and the IL-35 treated versus control were corrected for batch effects. The batch, which was orthogonal to treatment and cell type, was treated as a variable in an ANOVA model along with the variable of interest. The partial p value for the comparison of interest was then transformed to generate the significance score: $\text{score} = -\log_{10}(\text{p-value})$. This negative log transform allows the visualization of the differences between p-values which are not visible on the absolute scale. In the volcano plot the viewer can quickly see the degree of distinction a given gene may have from the body of data in both the magnitude of difference (log ratio) and the reliability of that difference (score). Probesets without a defined gene name were excluded from the graphs.

Assessment of iT_R stability in vivo. iT_{R35} or $TGF\beta$ iT_R were generated *in vitro* with $CD45.2^+$ T_{conv} cells to facilitate tracking of congenically marked cells. iT_R conversion was verified by qPCR analysis of signature genes (*Ebi3* and *IL12a* for iT_{R35} , *Foxp3* for $TGF\beta$ iT_R). 10^6 cells were adoptively transferred intravenously into $CD45.1^+$ C57BL/6 mice. Following 7, 15 or 25 days post-transfer, splenic iT_R cell number was determined by flow cytometric analysis of $CD45.2^+$ cells. The percentage of total cells injected compared to the number of cells recovered was used to calculate % recovery. To assess suppressive capacity, freshly purified T_{conv} cells were mixed at indicated ratios (T_{conv} : suppressor) with recovered iT_R cells and anti-CD3- + anti-CD28-coated latex beads for 72 h. Proliferation was determined by [3 H]-thymidine incorporation.

***Foxp3*^{-/-} rescue model.** The *Foxp3*^{-/-} rescue model was performed as described previously¹¹. Briefly, control treated (iT_R control), IL-35 treated (iT_{R35}) or $TGF\beta$ treated ($TGF\beta$ iT_R) cells were generated from FACS purified T_{conv} from wild type C57BL/6 or *Ebi3*^{-/-} mice. Cells were injected i.p. into 2-3 day old *Foxp3*^{-/-} mice. Recovery from disease was monitored weekly and reported as clinical score. Five macroscopic categories were utilized to generate a 6 point scoring

system. Mice were scored on the first 4 categories based on whether they showed (score of 1) or did not show (score of 0) the following characteristics: (1) body size runt, (2) tail scaly and/or with lesions, (3) ears small, scaly with or without lesions, and (4) eyelids scaly and/or not fully open. The final scoring parameter was monitoring the activity level of the mouse. A score of 0 was assigned if the mouse was normal. A score of 1 was assigned if the mouse's activity was moderately impaired, and a 2 assigned if the mouse was immobile. A combined score of 4 or greater was assigned moribund for longevity¹¹. Mice were euthanized 25 days post-transfer, spleen and LN cells counted, stained and cell numbers determined by flow cytometry. Lung, liver and ear pinna were prepared for H&E analysis and the severity of inflammation was assessed and scored in a blinded manner by an experienced veterinary pathologist. The scoring system used for assessing inflammation was based on a simple algorithm for expressing inflammatory infiltrates in the lungs, liver and ear. The scores allotted to these three tissues were 0-9, 0-11 and 0-8, respectively, giving a maximum possible total of 28. Scoring criteria for each organ was as follows. The lung score was based upon inflammation in the peribronchiolar region, perivascular region, or interstitium. A score of 0-3 was assigned to each category with 0 being minimal or no inflammation, and scores of 1, 2, or 3 indicative of <10%, 10-50%, or > 50%, respectively. The liver was scored based on 3 criteria. First, was the degree of portal tract inflammation with a score of 0 assigned to minimal or no inflammation. A score of 1, 2 or 3 was assigned if inflammation was associated with <25%, 25-75%, or >75% of the liver portal tracts, respectively. The second criteria related to portal/periseptal interface hepatitis. A focus of interface hepatitis associated with either a few or most of the portal tracts were scored 1 and 2, respectively. Two or more foci of interface hepatitis surrounding <50% or > 50% of the portal tracts or periseptae was scored 3 and 4 respectively. Third, foci of granulocytes and/or lymphocytes with or without necrotic hepatocytes that expand the sinusoid were considered foci of inflammation. The number of inflammatory foci in 10 contiguous 10x objective fields was counted and recorded as the average number of foci per 10x field and given

a score of 0 to 4. A score of 0 was assigned when sinusoidal foci of inflammatory cells was absent. One focus or less per 10x field, two to four foci per 10x field, five to ten foci per 10x field and more than ten foci per 10x field was scored 1, 2, 3 and 4 respectively. The ear pinna was similarly scored based on 2 parameters; the percent of the ear dermis with inflammatory infiltrates and the intensity of the dermal inflammation. For percent analysis, a score of 0 was assigned when the inflammatory cells in all segments were not beyond that of normal background level. A score of 1, 2, 3 or 4 was assigned when the average percent for the segments was <25%, 25-50%, 51-75% or >75%, respectively. The intensity of the inflammatory infiltrate in the dermis was assessed as being of a loose or dense nature. A score of 0 was assigned when inflammatory cells in the dermis was not beyond the normal background level. When all the inflammation was of the loose nature, a score of 1 was assigned. When there was a mixture of loose and dense inflammatory cell infiltrates a score of 2 was assigned when the loose form was dominant. A score of 3 was assigned when the dense form was dominant. A score of 4 was assigned when all of the inflammation was of a dense nature.

T_{reg} -mediated control of homeostatic expansion. Homeostasis assays were performed as described previously^{8, 12}. Briefly, naive Thy1.1⁺ T_{conv} cells were isolated by FACS and used as “responder” cells in adoptive transfer. Thy 1.2⁺ i T_{R35} or suppressed T_{conv} were generated as described above from wild-type or *Ebi3*^{-/-} mice and used as “suppressor” cells in adoptive transfer. T_{conv} cells (2×10^6) with or without suppressor cells (5×10^5) were resuspended in 0.5 ml of PBS plus 2% FBS, and were injected intravenously through the tail vein into *Rag1*^{-/-} mice. Mice were euthanized seven days post transfer, and splenocytes were counted, stained and analyzed by flow cytometry using antibodies against Thy1.1 and Thy1.2 (BD Bioscience). For each group, 6-10 mice were analyzed.

Inflammatory bowel disease model. The recovery model of IBD was used, with some modifications^{8, 13}. *Rag1*^{-/-} mice were injected intravenously with 4×10^5 wild-type or TGF β R.DN

T_{conv} cells to induce IBD. Upon clinical signs of disease, approximately four weeks post-transfer, mice were divided into appropriate experimental groups. Experimental groups received 7.5×10^5 iT_{R35} or control treated T_{conv} by intraperitoneal injection. All mice were weighed weekly and were euthanized 32 days post-transfer (eight weeks after the initial T_{conv} transfer). Colons were sectioned, fixed in 10% neutral buffered formalin and processed routinely, and 4-mm sections cut and stained with H&E or Alcian blue/Periodic acid Schiff. Pathology of the large intestine was scored blindly using a semiquantitative scale of zero to five as described previously¹⁴. In summary, grade 0 was assigned when no changes were observed; grade 1, minimal inflammatory infiltrates present in the lamina propria with or without mild mucosal hyperplasia; grade 2, mild inflammation in the lamina propria with occasional extension into the submucosa, focal erosions, minimal to mild mucosal hyperplasia and minimal to moderate mucin depletion; grade 3, mild to moderate inflammation in the lamina propria and submucosa occasionally transmural with ulceration and moderate mucosal hyperplasia and mucin depletion; grade 4 marked inflammatory infiltrates commonly transmural with ulceration, marked mucosal hyperplasia and mucin depletion, and multifocal crypt necrosis; grade 5, marked transmural inflammation with ulceration, widespread crypt necrosis and loss of intestinal glands.

MOG EAE disease model. The EAE disease model was performed as described previously¹¹. Briefly, EAE was induced with MOG₃₅₋₅₅ (MEVGWYRSPFSRVVHLYRNGK; produced at St. Jude Hartwell Center for Biotechnology) by injecting 50 μ g of MOG₃₅₋₅₅ emulsified in complete Freund's adjuvant containing 0.2 mg of H37Ra mycobacterium tuberculosis (Difco Laboratories) in 50 μ l s.c. in each hind flank. 200 ng of *Bordetella pertussis* toxin (Difco Laboratories) was administered i.v. on days 0 and 2¹⁵. Clinical scoring was as follows: 1, limp tail; 2, hind limb paresis or partial paralysis; 3, total hind limb paralysis; 4, hind limb paralysis and body/front limb paresis/paralysis; 5, moribund. In all experiments that involved EAE disease induction 5 mice per group were used.

B16 and MC38 tumor models. For IL-35 expression analyses, $Foxp3^{gfp}$ or $Ebi3^{-/-}Foxp3^{gfp}$ mice were inoculated with B16 melanoma or MC38 colorectal adenocarcinoma cells. The B16 melanoma model was performed as described previously¹¹. MC38 colorectal adenocarcinoma cells (a gift from Drs. Alan Korman and Mark Selby, Medarex/BMS^{16,17}) were cultured in DMEM+10% FBS, washed and resuspended in PBS prior to s.c. injection of 2×10^6 cells on the right flank. For T cell adoptive transfer experiments using the B16 melanoma model, $Rag1^{-/-}$ mice received indicated cells via the tail vein on day -1 of experiment. Wild type or $Ebi3^{-/-}$ naïve $CD4^+CD25^-$ (9×10^6 /mouse) and $CD8^+$ T cells (6×10^6 /mouse) alone or in combination with natural T_{regs} or iT_{R35} cells (10^6 /mouse) were adoptively transferred into mice. B16-F10 melanoma was a gift from Mary Jo Turk (Dartmouth College, Hanover, NH) and was passaged intradermally (i.d.) in C57/Bl6 mice 5 times to ensure reproducible growth. B16 cells were cultured in RPMI 1640 containing 7.5% FBS and washed three times with RPMI prior to injections if viability exceeded 96%. $Rag1^{-/-}$ mice were injected with 120,000 cells on the right flank i.d. B16 tumor diameters were measured daily with calipers and reported as mm^3 ($a^2 \times b/2$, where a is the smaller caliper measurement and b the larger)^{18,19}. For all experiments, B16 tumors were excised at 15-17 days when tumor size was 5-10 mm in diameter. MC38 tumors were excised at 12 days when tumor size was 5-15 mm in diameter. All tumor infiltrating lymphocytes (TILs) were isolated by first generating a single cell suspension by teasing tumor between frosted microscope slides. Lymphocytes were obtained from the 40%/80% Percoll gradient interface. Lymphocytes were stained with anti-CD4 and anti-Thy1.1 and anti-Thy1.2 mAbs as necessary and passed through a 40 μ m cell strainer prior to cell sorting.

***Trichuris muris* Infections.** *Trichuris muris* was maintained in genetically susceptible animals and isolation of *Trichuris muris* eggs was performed as described previously²⁰. Mice were infected orally with 30 embryonated *Trichuris muris* eggs and sacrificed on day 14 post-infection. Single cell suspensions from mesenteric lymph node, spleen and combined lamina

propria + intraepithelial lymphocyte (LPL+IEL) compartments of the small and large intestine were prepared and stained with fluorochrome-labeled anti-CD4 antibodies. CD4⁺ FoxP3⁺ and CD4⁺ FoxP3⁻ cell fractions were enriched using a FACS DIVA cell sorter and subject to mRNA isolation and Real Time PCR analysis as described above.

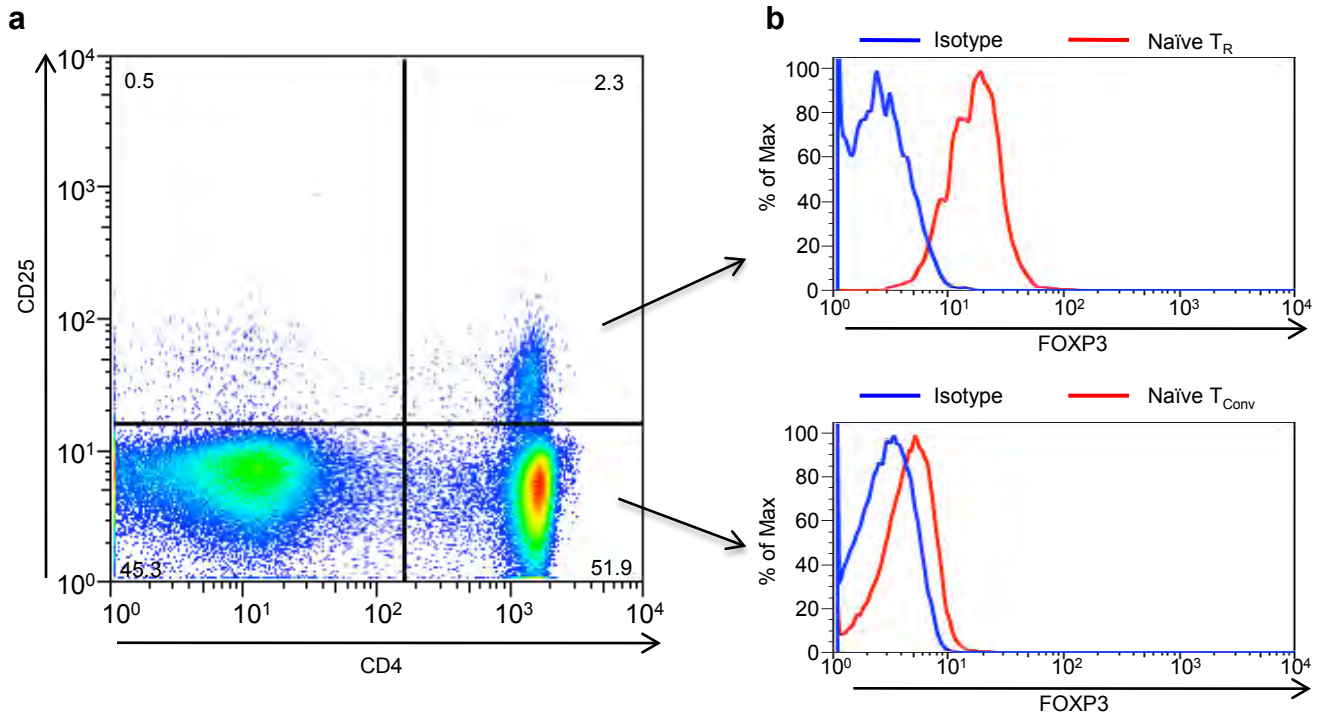
Statistical Analysis. Statistical significance was determined in all figures using an unpaired T test unless otherwise noted in figure legends. In select figures (where noted in legends) statistical analysis was determined using Wilcoxon matched pairs test. All statistics were determined with GraphPad Prism software (San Diego, CA).

References.

1. Fahlen, L. et al. T cells that cannot respond to TGF-beta escape control by CD4(+)CD25(+) regulatory T cells. *J Exp Med* 201, 737-746 (2005).
2. Hill, J.A. et al. Foxp3 transcription-factor-dependent and -independent regulation of the regulatory T cell transcriptional signature. *Immunity* 27, 786-800 (2007).
3. Groux, H. et al. A CD4⁺ T-cell subset inhibits antigen-specific T-cell responses and prevents colitis. *Nature* 389, 737-742 (1997).
4. Roncarolo, M.G. et al. Interleukin-10-secreting type 1 regulatory T cells in rodents and humans. *Immunol Rev* 212, 28-50 (2006).
5. Barrat, F.J. et al. In vitro generation of interleukin 10-producing regulatory CD4(+) T cells is induced by immunosuppressive drugs and inhibited by T helper type 1 (Th1)- and Th2-inducing cytokines. *J Exp Med* 195, 603-616 (2002).
6. Kemper, C. et al. Activation of human CD4⁺ cells with CD3 and CD46 induces a T-regulatory cell 1 phenotype. *Nature* 421, 388-392 (2003).
7. Vignali, D.A. & Vignali, K.M. Profound enhancement of T cell activation mediated by the interaction between the TCR and the D3 domain of CD4. *J Immunol* 162, 1431-1439 (1999).
8. Collison, L.W. et al. The inhibitory cytokine IL-35 contributes to regulatory T-cell function. *Nature* 450, 566-569 (2007).
9. Huang, C.T. et al. Role of LAG-3 in regulatory T cells. *Immunity* 21, 503-513 (2004).

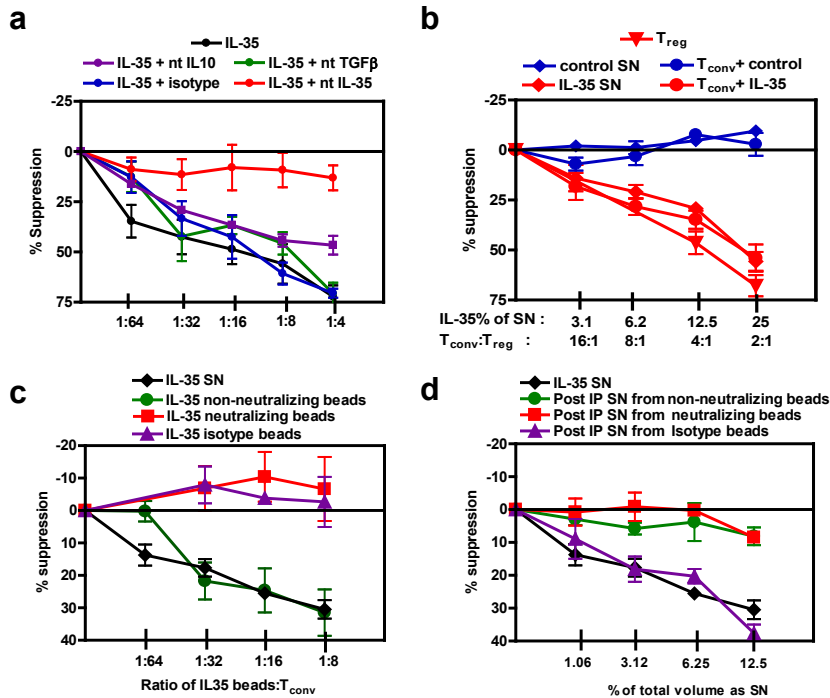
10. Roche, D .M. & Durbin, B . A pproximate v ariance-stabilizing t ransformations for g ene-expression microarray data. *Bioinformatics* 19, 966-972 (2003).
11. Workman, C.J. *et al.* In vivo Treg Suppression Assays. *Regulatory T cells: Methods and Protocols. In Press.* (2010).
12. Workman, C.J. *et al.* Lymphocyte activation gene-3 (CD223) regulates the size of the expanding T cell population following antigen activation in vivo. *J Immunol* 172, 5450-5455 (2004).
13. Mottet, C., Uhlig, H.H. & Powrie, F. Cutting edge: cure of colitis by CD4+CD25+ regulatory T cells. *J Immunol* 170, 3939-3943 (2003).
14. Asseman, C., Mauze, S., Leach, M.W., Coffman, R.L. & Powrie, F. An essential role for interleukin 10 in the function of regulatory T cells that inhibit intestinal inflammation. *J Exp Med* 190, 995-1004 (1999).
15. Selvaraj, R.K. & Geiger, T.L. Mitigation of experimental allergic encephalomyelitis by TGF-beta induced Foxp3+ regulatory T lymphocytes through the induction of anergy and infectious tolerance. *J Immunol* 180, 2830-2838 (2008).
16. Kocak, E. *et al.* Combination therapy with anti-CTL antigen-4 and anti-4-1BB antibodies enhances cancer immunity and reduces autoimmunity. *Cancer Res* 66, 7276-7284 (2006).
17. Peggs, K.S., Quezada, S.A., Chambers, C.A., Korman, A.J. & Allison, J.P. Blockade of CTLA-4 on both effector and regulatory T cell compartments contributes to the antitumor activity of anti-CTLA-4 antibodies. *J Exp Med* 206, 1717-1725 (2009).
18. Turk, M.J. *et al.* Concomitant tumor immunity to a poorly immunogenic melanoma is prevented by regulatory T cells. *J Exp Med* 200, 771-782 (2004).
19. Zhang, P., Cote, A.L., de Vries, V.C., Usherwood, E.J. & Turk, M.J. Induction of postsurgical tumor immunity and T-cell memory by a poorly immunogenic tumor. *Cancer Res* 67, 6468-6476 (2007).
20. Artis, D. *et al.* The IL-27 receptor (WSX-1) is an inhibitor of innate and adaptive elements of type 2 immunity. *J Immunol* 173, 5626-5634 (2004).

Supplementary Figure 1



Supplementary Figure 1: Purity of human T_{reg} Human T_{conv} and T_{reg} were purified from umbilical cord blood by FACS based on cell surface expression of CD4 and CD25. Purified cells were subsequently fixed, permeabilized and stained for FoxP3. Representative profiles of cord blood purification (a) Foxp3 expression in CD4⁺ cells gated on CD25⁺ (top panel) or CD25⁻ (bottom panel).

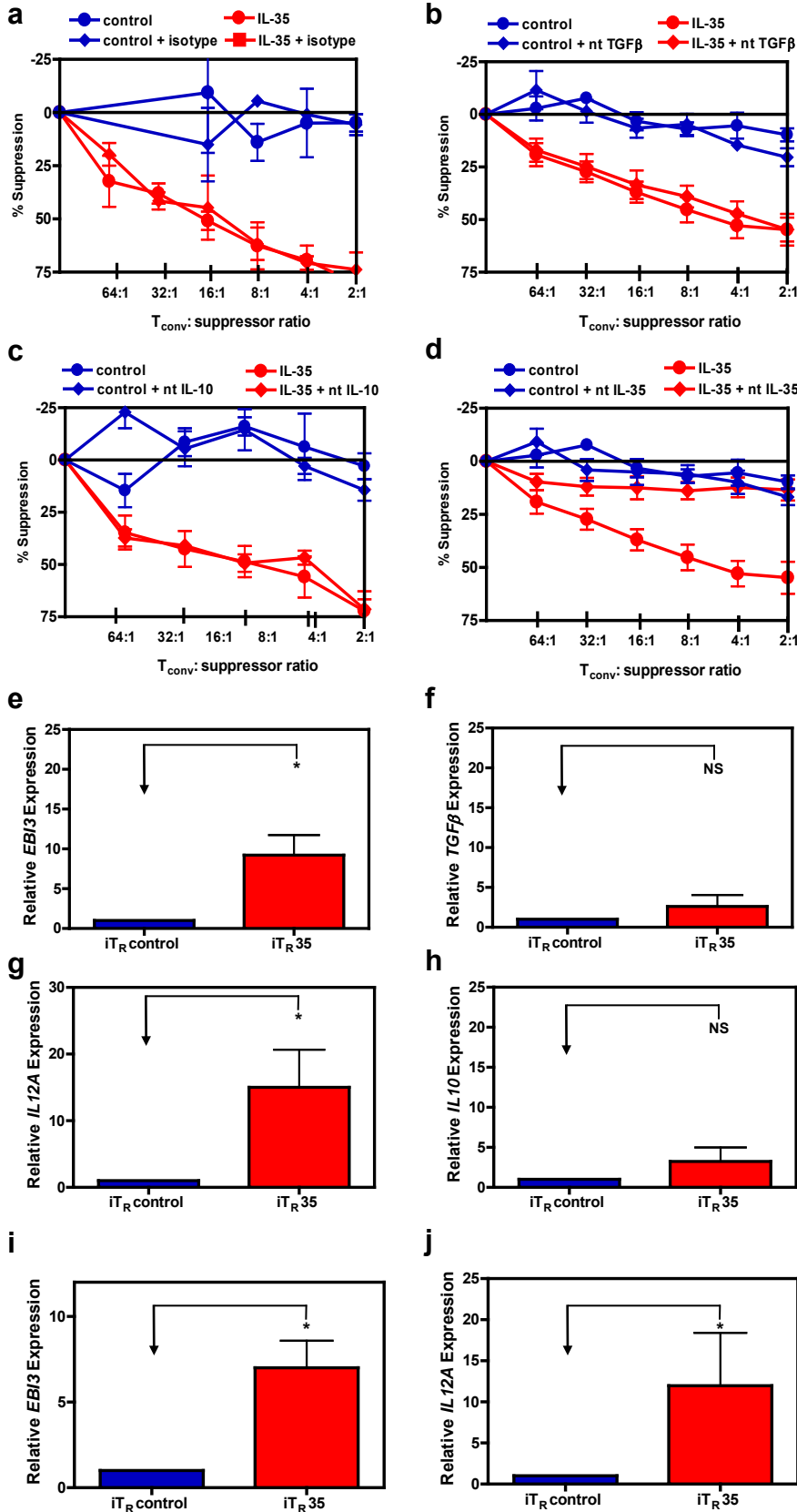
Supplementary Figure 2



Supplementary Figure 2 : IL-35 suppressive capacity and validation of human IL-35 SN.

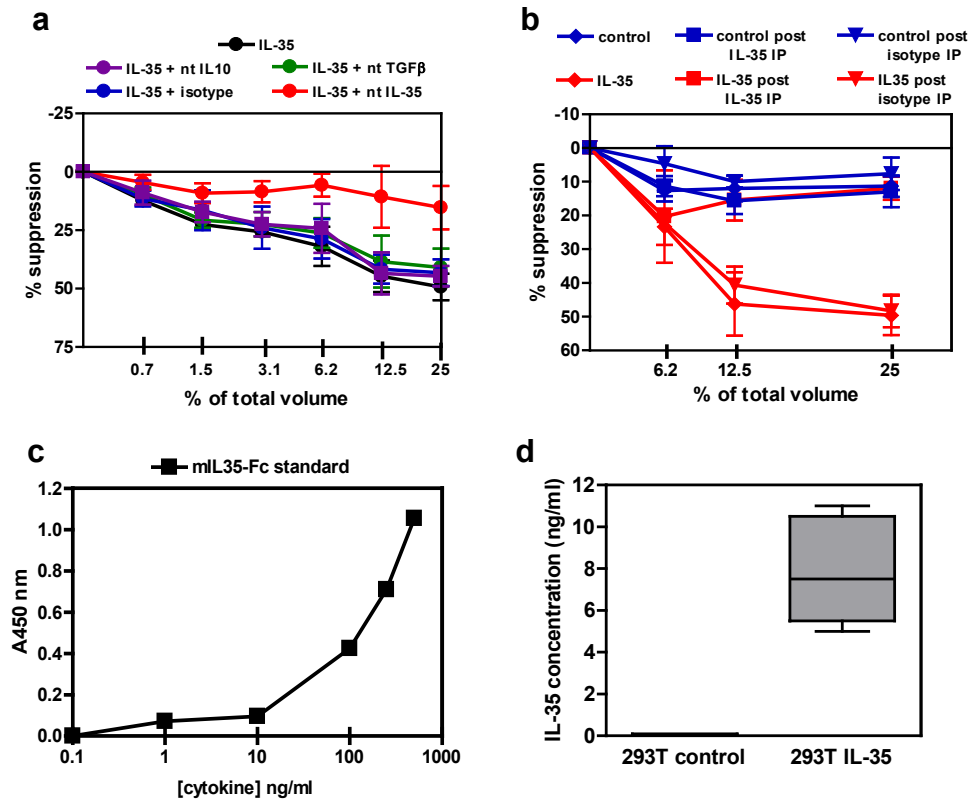
(a) T_{conv} cells were activated in the presence of IL-35 or control supernatant, at 25% of total culture volume. During conversion with cytokines, suppression assays were supplemented with neutralizing IL-10, TGF β , or IL-35. Following conversion, cells were cultured with freshly purified T_{conv} at indicated ratios and suppressive capacity determined. Data represents an average of 5 independent experiments done in duplicates. The p values comparing IL-35 neutralizing antibody compared to IL-35 only were significant at all concentrations and ranged between 0.002-0.04 (b) T_{conv} sorted from cord blood were activated in the presence of IL-35 SN, control SN, *in vitro* expanded Tregs, iT_R35 and iT_Rcontrol and proliferation determined by [³H]-thymidine incorporation. Data represents an average of 3 independent experiments done in duplicates. The p values ranged between 0.144-0.166 at all concentrations for the suppression capacity of iT_R35 compared to *in vitro* activated Tregs. (c-d) Isotype control, neutralizing Ab, and non-neutralizing Ab were incubated with IL-35 SN or control SN and IL-12a and then coupled with protein G beads.(c) The protein G coupled beads were then incubated with T_{conv} cells activated in presence of α CD3 and α CD28. Data represents an average of 4 independent experiments done in duplicates. The p values were significant (0.0072-<0.0001) between IL-35 SN and IL-35 neutralizing beads at all concentrations except 1:64. The p values (0.5-0.91) at all concentrations were not significant between IL-35 SN and IL-35 non neutralizing beads. (d) IL-35 depleted SN (noted as post IP SN) was also cultured with T_{conv} cells to demonstrate loss of IL-35 activity. Counts per minute of T_{conv} cells activated alone were 76,000-430,000 (a) 11,000-293,000 (c). Data represents an average of 4 independent experiments done in duplicates. The p values were significant at all concentrations, except for 1.08, for IL-35 SN and Post IP SN from non neutralizing beads (0.01-0.0013) and IL-35 SN and Post IP SN from neutralizing beads (0.018-<0.0001). IL-35 SN was used as a control throughout.

Supplementary Figure 3



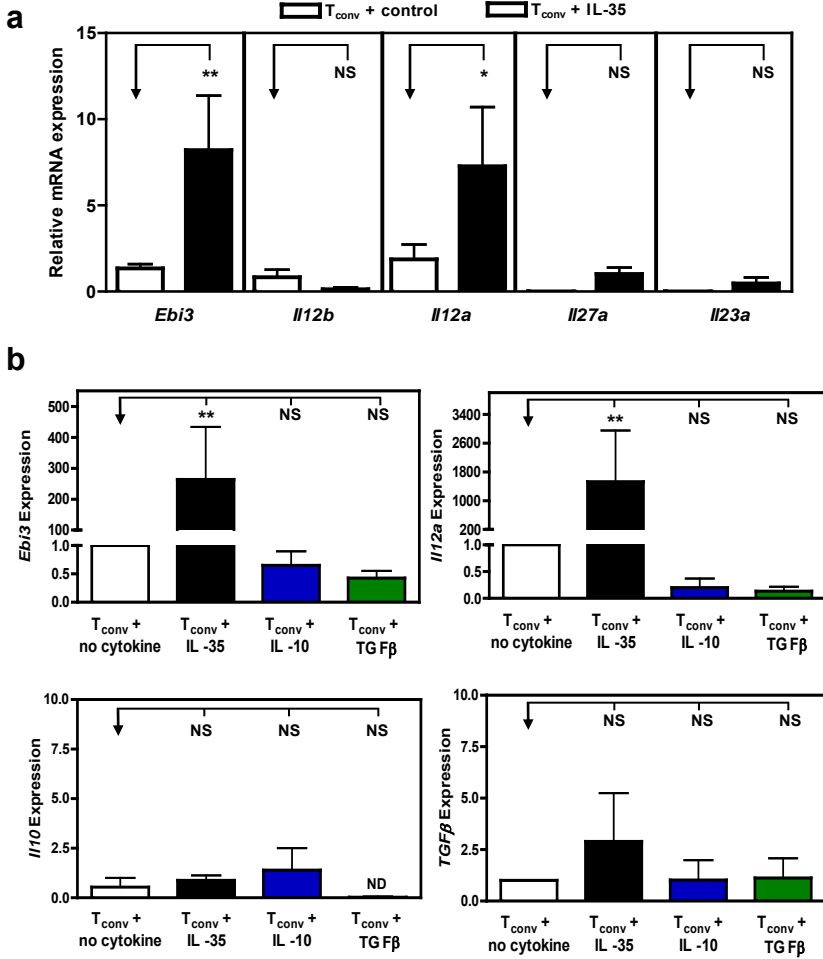
Supplementary Figure 3: IL-35 is sufficient and required for generation of human iT_R35. (a-d) Human T_{conv} cells were activated in the presence of IL-35 or control SN at 25% of total culture volume. Following conversion with cytokine, suppression assays were supplemented with neutralizing mAbs against IL-10, TGFβ, or IL-35 to assess their requirement for indicated cytokines to mediate suppression. Only the addition of IL-35 neutralizing antibody resulted in loss of suppressive capacity (p values ranging from 0.0003-0.0066 at all concentrations except at 1:64). (e-j) Human control or IL-35 treated cord blood (e-h) or PBMC-derived (i-j) T_{conv} cells were generated by 9 day culture with either control or IL-35 SN. Following conversion, RNA was isolated, cDNA generated and qPCR analysis performed. Relative EB13, IL12A, IL10 and TGFβ expression. Data represent the mean + SEM of 3 independent experiments. [* p < 0.05, NS = not significant]

Supplementary Figure 4



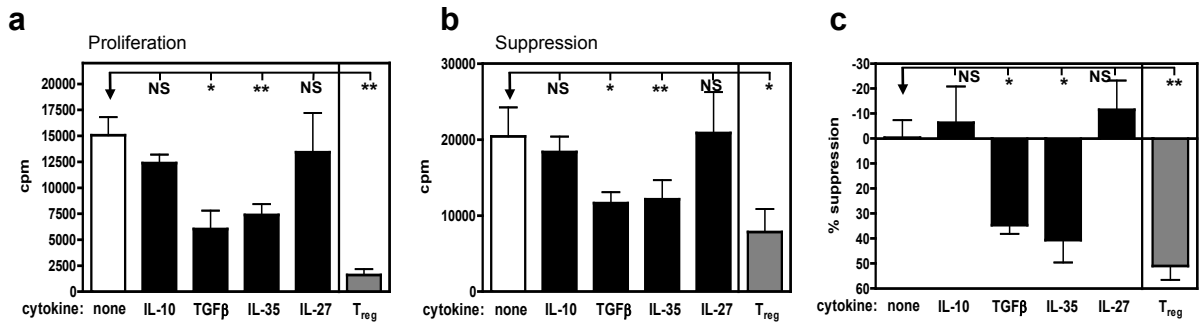
Supplementary Figure 4: SN-derived murine IL-35 is suppressive and specific. (a) IL-35 SN was titrated, in combination with the indicated isotype control or neutralizing antibodies, into a suppression assay with freshly purified murine T_{conv} cells. The data represents an average of three experiments done in duplicates. The addition of IL-35 neutralizing antibody resulted in loss of suppressive capacity (p values ranged between <0.0001 - <0.0032). (b) Control or IL-35 SN was cultured with isotype or anti-p35 coupled Protein G beads. Following immunoprecipitation, post-IP SN (or freshly generated SN) was added to suppression assays, as described in a, to determine suppressive capacity. Proliferation was determined by [3 H]-thymidine incorporation. Counts per minute of T_{conv} cells activated alone were 21,000-64,000 (a) 14,000-38,000 (b). Data represent the mean + SEM of 3-5 independent experiments. (c-d) ELISA quantification of IL-35 in control and IL-35 transfected 293Ts. Concentration was determined using mIL-35:Fc chimeric protein (c). Average IL-35 detected in 5 independently generated 293T transfectants (d).

Supplementary Figure 5



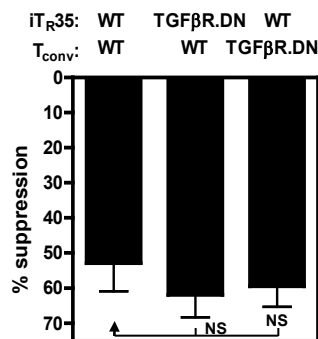
Supplementary Figure 5: IL-35 treatment, but not control, IL-10, or TGFβ induces IL-35 expression (a) Murine T_{conv} cells were activated in the presence of control or IL-35 SN for 72 h. Following conversion, RNA was isolated, cDNA generated and qPCR analysis performed to determine relative expression of *Ebi3*, *Il12b*, *Il12a*, *Il27a*, and *Il23a*. (b) T_{conv} purified by FACS from C57BL/6 mice were treated with indicated cytokines for 72 h in the presence of anti-CD3 + anti-CD28 coated latex beads. RNA was extracted and cDNA generated from purified cells. Relative *Ebi3*, *p35*, *IL-10* and *TGFβ* expression. Data represent the mean SEM of 3-5 independent experiments. [* $p < 0.05$, ** $p < 0.005$, NS = not significant]

Supplementary Figure 6



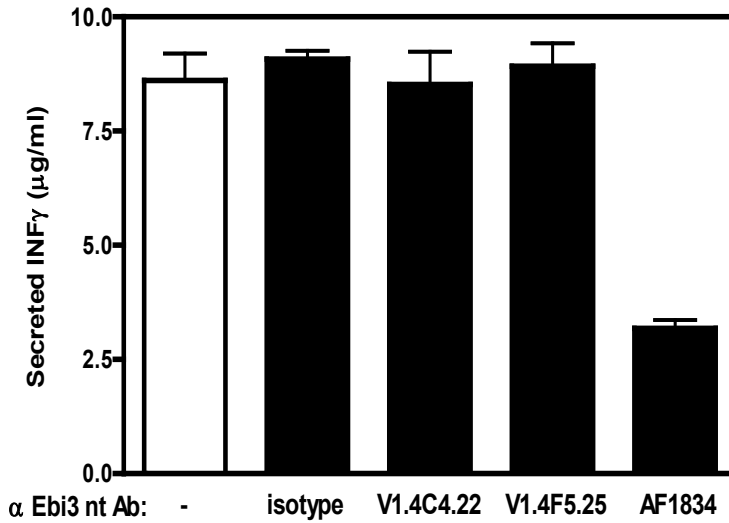
Supplementary Figure 6: Treatment with mIL-35 and TGFβ, but not control cytokines, renders murine T cells hypoproliferative and suppressive. Wild-type murine T_{conv} cells were activated in the presence of indicated cytokines at 25% of total culture volume for SN and 100ng/ml for recombinant cytokines. (a) Following treatment with cytokines, proliferative capacity was determined by activating cells with anti-CD3/anti-CD28 coated latex beads. Cultures were pulsed with [³H]-thymidine for the final 8 h of a 72 h assay. (b-c) Following cytokine treatment, cells were cultured at a 4:1 ratio in suppression assays with freshly purified T_{conv} cells to determine suppressive capacity. Proliferation was determined by [³H]-thymidine incorporation. 3 experiments with similar cpm are depicted in b. Average % suppression for all data sets in c. Counts per minute of T_{conv} cells activated alone were 14,000-29,000 (c). Data represent the mean + SEM. of 3 independent experiments. [* p < 0.05, ** p < 0.005, NS = not significant]

Supplementary Figure 7



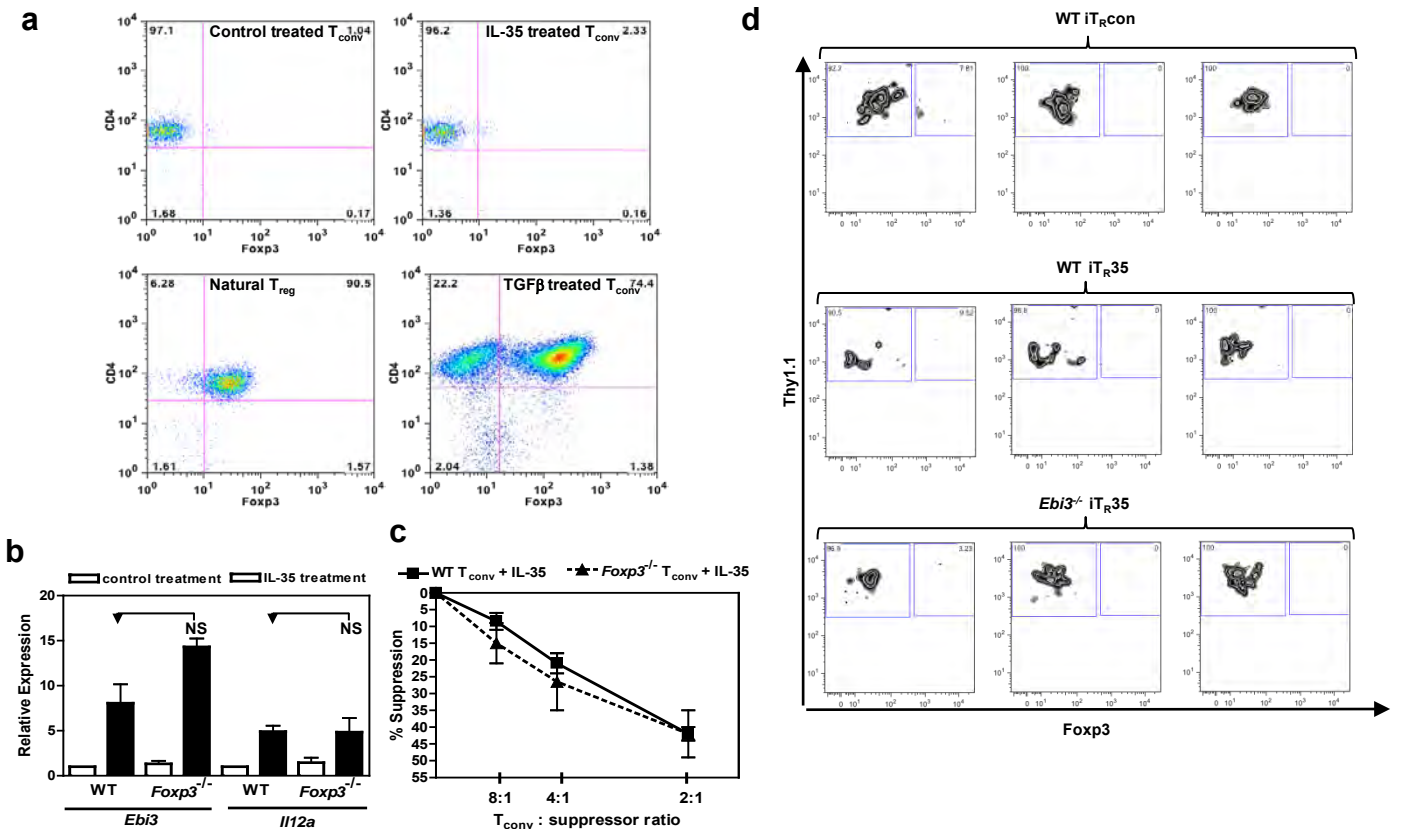
Supplementary Figure 7. TGFβ is not required for conversion or function of murine iT_{R35}. iT_{R35} from wild-type C57BL/6 (WT) or TGFβR.DN mice were activated in the presence of IL-35, at 25% of total culture volume, for 72 h to generate suppressive cells. Cells were re-purified and mixed at 4:1 ratio (T_{conv}: suppressor) with T_{conv} from WT or TGFβR.DN mice and proliferation was determined. Counts per minute of T_{conv} cells activated alone were 24,000-51,000. Data represent the mean + SEM of 4 independent experiments. [NS = not significant]

Supplementary Figure 8



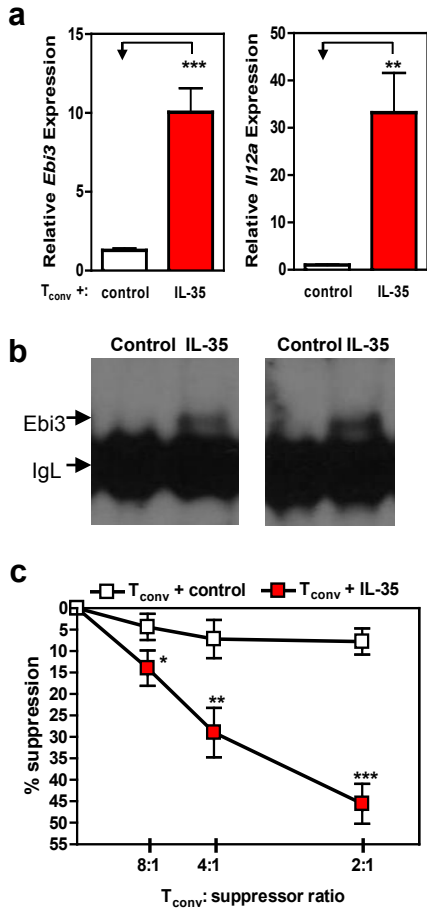
Supplementary Figure 8: IL-27 bioassay demonstrates that anti-Ebi3 mAbs V1.4C4.22 and V1.4F5.2 are IL-35 specific. Purified murine T_{conv} cells were activated with anti-CD3 and anti-CD28 mAb in the presence of rIL-27 and rIL-12 (50ng/ml) and neutralizing anti-IL-2 mAb. IL-27 activity was measured by determining IFN γ secretion in the presence of anti-IL-35 mAbs V1.4C4.22 and V1.4F5.25 or neutralizing anti-Ebi3 mAb AF1834, at a final concentration of 10 $\mu\text{g/ml}$.

Supplementary Figure 9



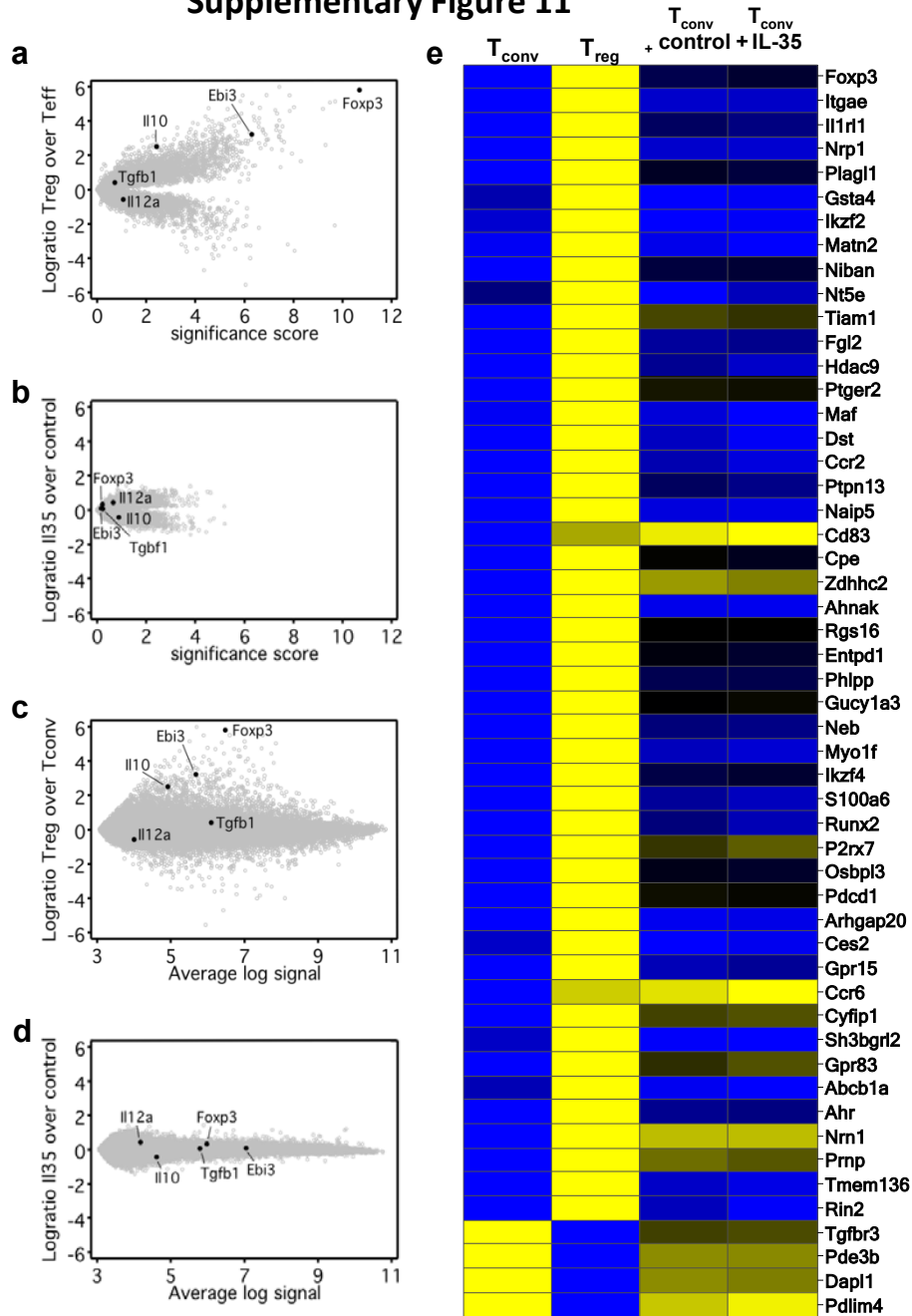
Supplementary Figure 9. IL-35 treated cells do not express or require Foxp3 for murine iT_R35 conversion. (a) T_{conv} purified by FACS from *Foxp3*^{9fp} mice were activated with anti-CD3 + anti-CD28 coated latex beads in the presence of control protein (top left panel) IL-35 (top right panel) for 3 days or under Th3 inducing conditions (bottom right panel) for 5 days. Foxp3 induction was monitored and compared to that of purified natural T_{regs}. (b-c) Murine control or IL-35 treated T_{conv} cells were generated from 3 week old wild type or *Foxp3*^{-/-} T_{conv} cells. (b) RNA was isolated, cDNA generated and qPCR performed to determine *Ebi3* and *Il12a* expression. (c) IL-35 treated T_{conv} from wild type or *Foxp3*^{-/-} were mixed at indicated ratios (T_{conv}: suppressor) with freshly purified T_{conv} and anti-CD3- + anti-CD28-coated latex beads for 72 h. Proliferation was determined by [³H]-thymidine incorporation. Counts per minute of T_{conv} cells activated alone were 23,000-37,000 (c). (d) Homeostatic expansion was monitored by i.v. injection of Thy1.2⁺ T_{conv} cells alone or with Thy1.1⁺ Foxp3^{9fp} (wild type or *Ebi3*^{-/-}) iT_Rcontrol or iT_R35 cells (as regulatory cells) into *Rag1*^{-/-} mice. Seven days after transfer, Foxp3^{9fp} induction was monitored in iT_Rcontrol or iT_R35 cells by flow cytometry. Data represent the mean + SEM of 3 independent experiments. [NS = not significant]

Supplementary Figure 10



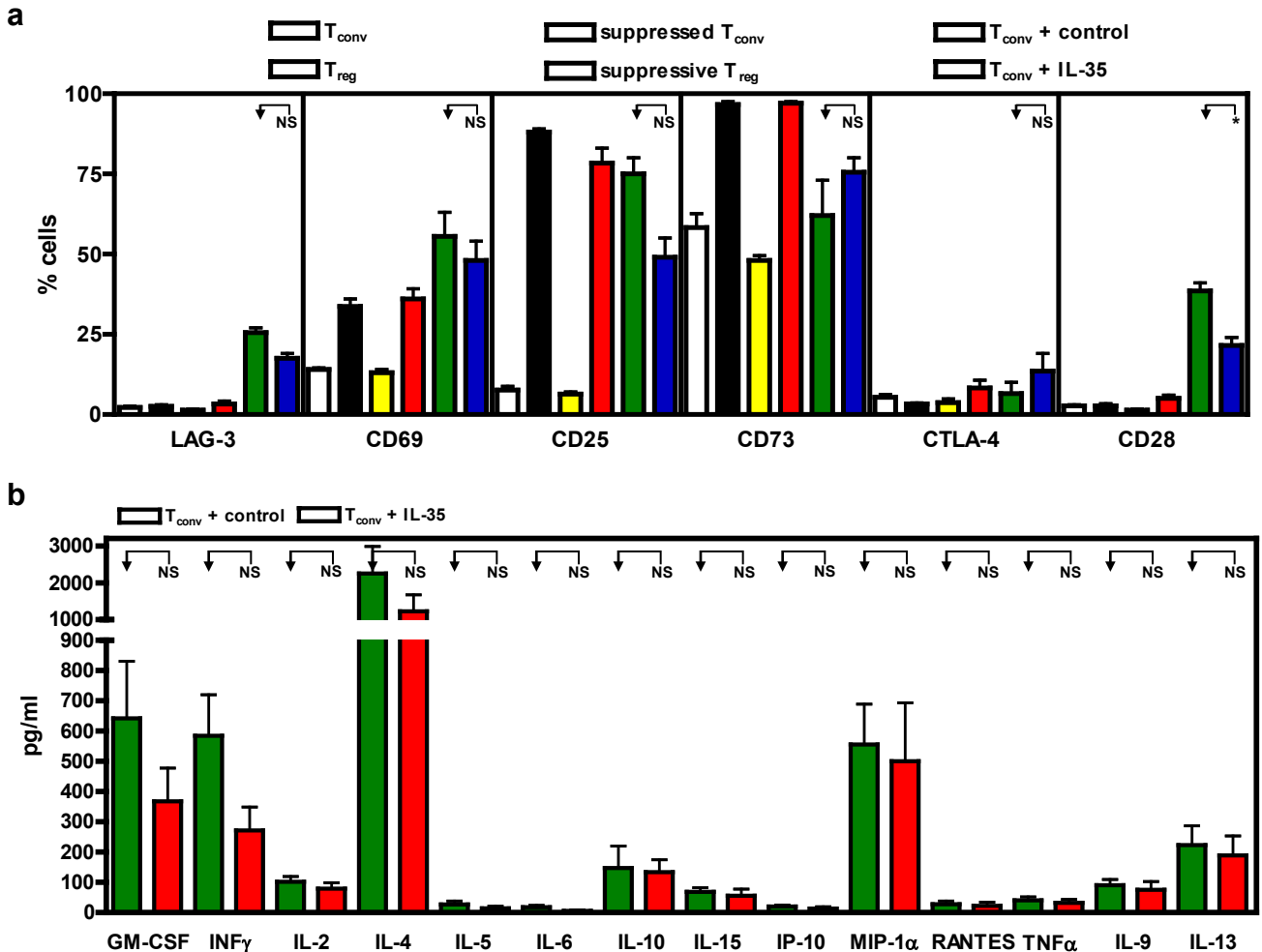
Supplementary Figure 10: Validation of the IL-35 treated T_{conv} cell phenotype. Murine T_{conv} cells were cultured with control or IL-35 protein and anti-CD3- + anti-CD28-coated latex beads for 72 h. IL-35 production was determined by (a) Relative *Ebi3* (left panel) and *Il12a* (right panel) mRNA expression. (b) Immunoprecipitation and Western blotting after thorough washing and culture for an additional 24 h. Two representative blots are shown. (c) T_{conv} cells were mixed at indicated ratios (T_{conv} :suppressor) with cytokine treated T_{conv} and anti-CD3- + anti-CD28-coated latex beads for 72 h. Proliferation was determined by [3 H]-thymidine incorporation. Counts per minute of T_{conv} cells activated alone were 19,000-44,000 (c). Data represent the mean \pm SEM of 3-5 independent experiments. [* $p < 0.05$, ** $p < 0.005$, *** $p < 0.001$]

Supplementary Figure 11



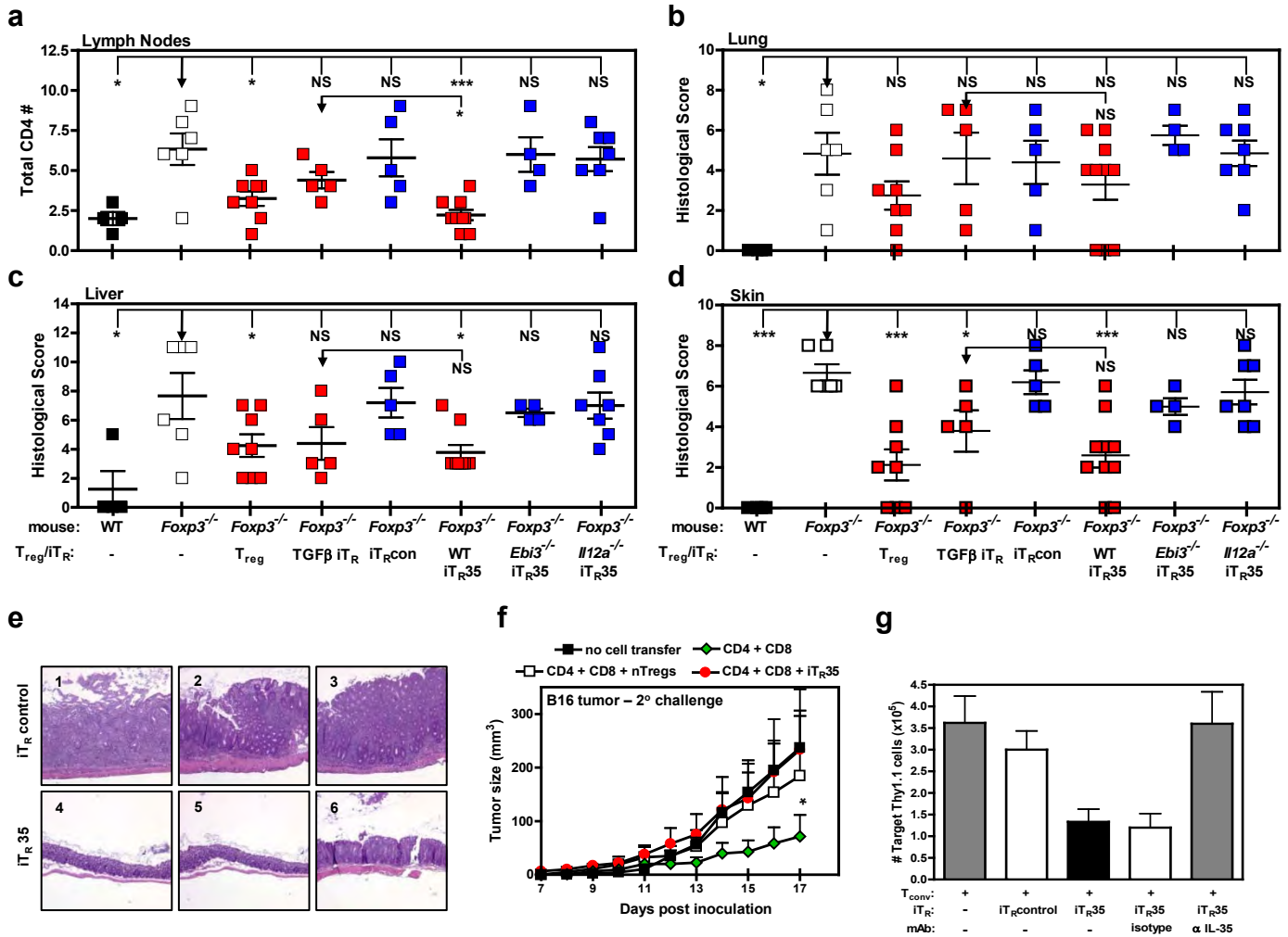
Supplementary Figure 11: Affymetrix analyses of control and IL-35 treated T_{conv} . Murine T_{conv} cells were cultured with control or IL-35 protein and anti-CD3- + anti-CD28-coated latex beads for 72 h. Analyses of these samples, compared to freshly purified T_{conv} or T_{reg} was determined. (a-b) Magnitude and abundance plots (MA plots) show the relative change in expression on the y axis by the logratio of (a) T_{reg} vs over T_{conv} and (b) IL-35 treated cells over control treated cells compared to their average log signals on the x axis. (c) A horizontal volcano plot visualizing the magnitude of change between T_{conv} and T_{reg} for each probeset on the microarray. The log2ratio of T_{reg} over T_{conv} expression for each probeset is on the y axis and the significance score on the x axis is the $-\log_{10}(p \text{ value})$ (d) A horizontal volcano plot comparing IL-35 and control treated T_{conv} cells (e) A heat map comparing the mean expression of 52 genes that differentiate T_{regs} from T_{conv} cells. The relative score from 0 to 1 is plotted as blue if zero, black if 0.5 and yellow if 1. Intermediate values are shaded. Data represent at least 5 independent experiments.

Supplementary Figure 12



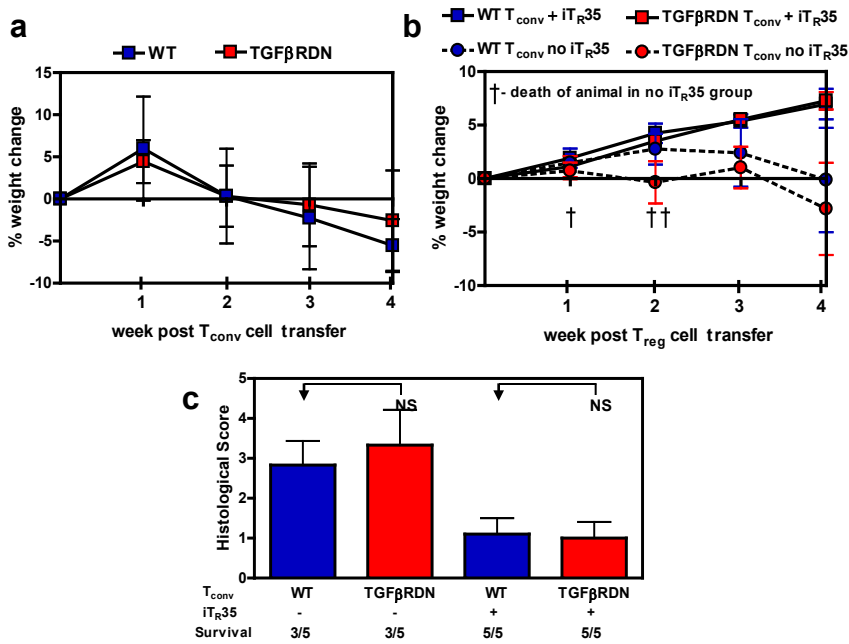
Supplementary Figure 12: Murine iT_{Rcon} and iT_{R35} express similar levels of cell surface and secreted molecules. $iT_{Rcontrol}$ and iT_{R35} were generated by 3 day culture with control or IL-35 SN at 25% of total cell culture volume. (a) Murine T_{conv} cells were cultured with T_{regs} and anti-CD3- + anti-CD28-coated latex beads for 72 h. Following culture, suppressed T_{conv} and suppressive T_{regs} were re-purified for comparison to T_{conv}, T_{reg}, $iT_{Rcontrol}$, and iT_{R35} . (a) All cells were stained with indicated antibodies and frequency of expression was determined by flow cytometric analysis. (b) Cells were cultured for 24 h and supernatants collected and analyzed for indicated soluble factors by Milliplex analysis. Data represent the mean + SEM of 4-6 independent experiments. [* p < 0.05, NS = not significant]

Supplementary Figure 13



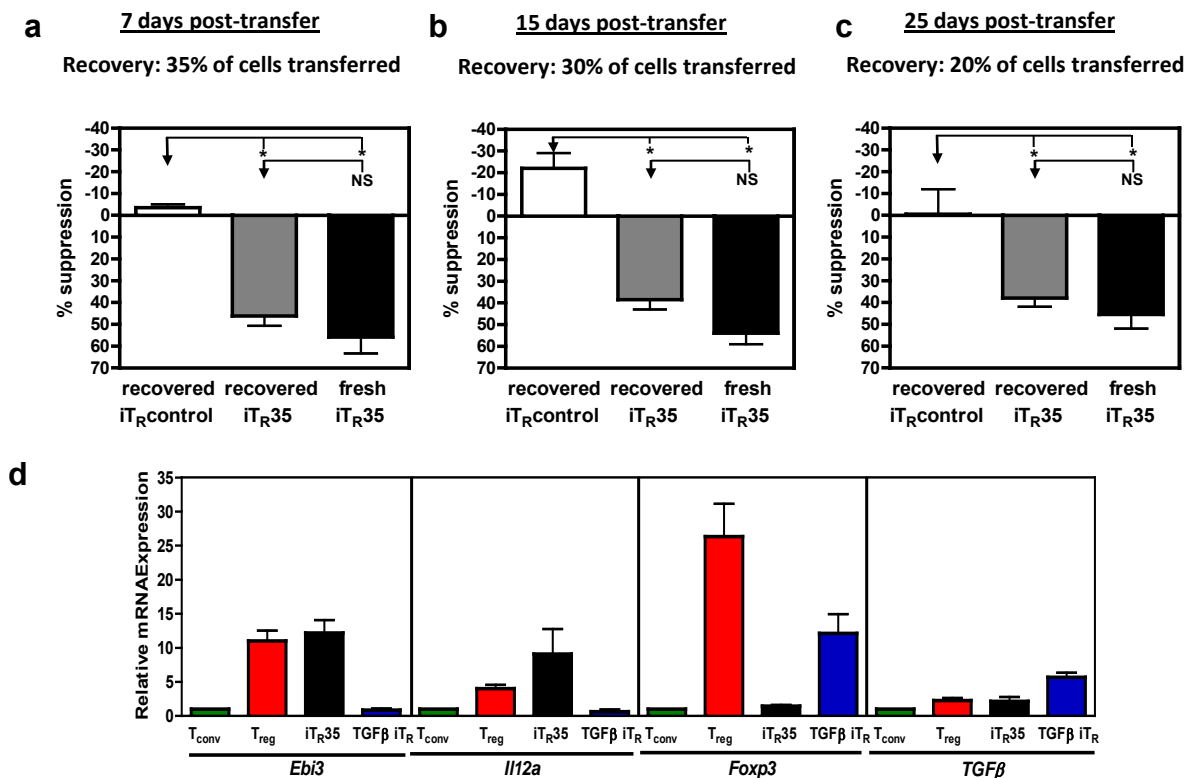
Supplementary Figure 13: Murine iT_R35 are suppressive *in vivo*. (a-d) Control treated (iT_Rcontrol), IL-35 treated (iT_R35) or TGFβ treated (TGFβ iT_R) cells were generated from FACS purified T_{conv} from wild type C57BL/6, *Ebi3*^{-/-} or *I12a*^{-/-} mice. Cells were injected i.p. into 2-3 day old *Foxp3*^{-/-} mice. Recovery from disease was monitored and reported by reduction in (a) lymph node CD4⁺ T cell number as determined by flow cytometric analysis (b) lung histological score (c) liver histological analysis (d) skin histological analysis. To induce IBD, *Rag1*^{-/-} mice received T_{conv} cells via the tail vein. After 3–4 weeks, mice developed clinical symptoms of IBD and were given iT_Rcontrol or iT_R35 cells. *Rag1*^{-/-} mice received CD4⁺CD25⁻CD45RB^{hi} T_{conv} cells with or without indicated T_{reg} cells via the tail vein. After 8 weeks, histological sections of representative colons from each group were stained with H&E. Representative iT_Rcontrol cell transfer (images 1-3) or iT_R35 cell transfer (images 4-6). (f) *Rag1*^{-/-} mice received indicated cells via the tail vein on day -1 of experiment. On day 0, the mice were injected with 120,000 B16 cells i.d. in the right flank. Tumor diameter was measured daily for 15 days. Primary tumors were excised and mice received a secondary challenge tumor on the left flank and tumors were measured daily. Mean tumor size at all timepoints was statistically significant between groups receiving CD4 + CD8 and CD4 + CD8 + iT_R35. iT_Rcontrol or iT_R35 were generated from FACS purified T_{conv} from C57BL/6 or *Ebi3*^{-/-} (Thy1.2) or B6.PL (Thy1.1) mice. (g) Homeostatic expansion was monitored by i.v. injection of Thy1.1⁺ T_{conv} cells alone or with Thy1.2⁺ iT_Rcontrol or iT_R35 cells (as regulatory cells) into *Rag1*^{-/-} mice. Mice were given anti-IL35 neutralizing mAb or isotype control via intraperitoneal injections on day 0 (500μg/mouse), day 3 (250μg/mouse), and day 6 (250μg/mouse). Seven days post-transfer, the number of splenic Thy1.1⁺ target T_{conv} were determined by flow cytometry. Data represent the mean ± SEM of 5-12 mice per group from at least 2 independent experiments. [* p < 0.05, ** p < 0.005, *** p < 0.001, NS = not significant]

Supplementary Figure 14



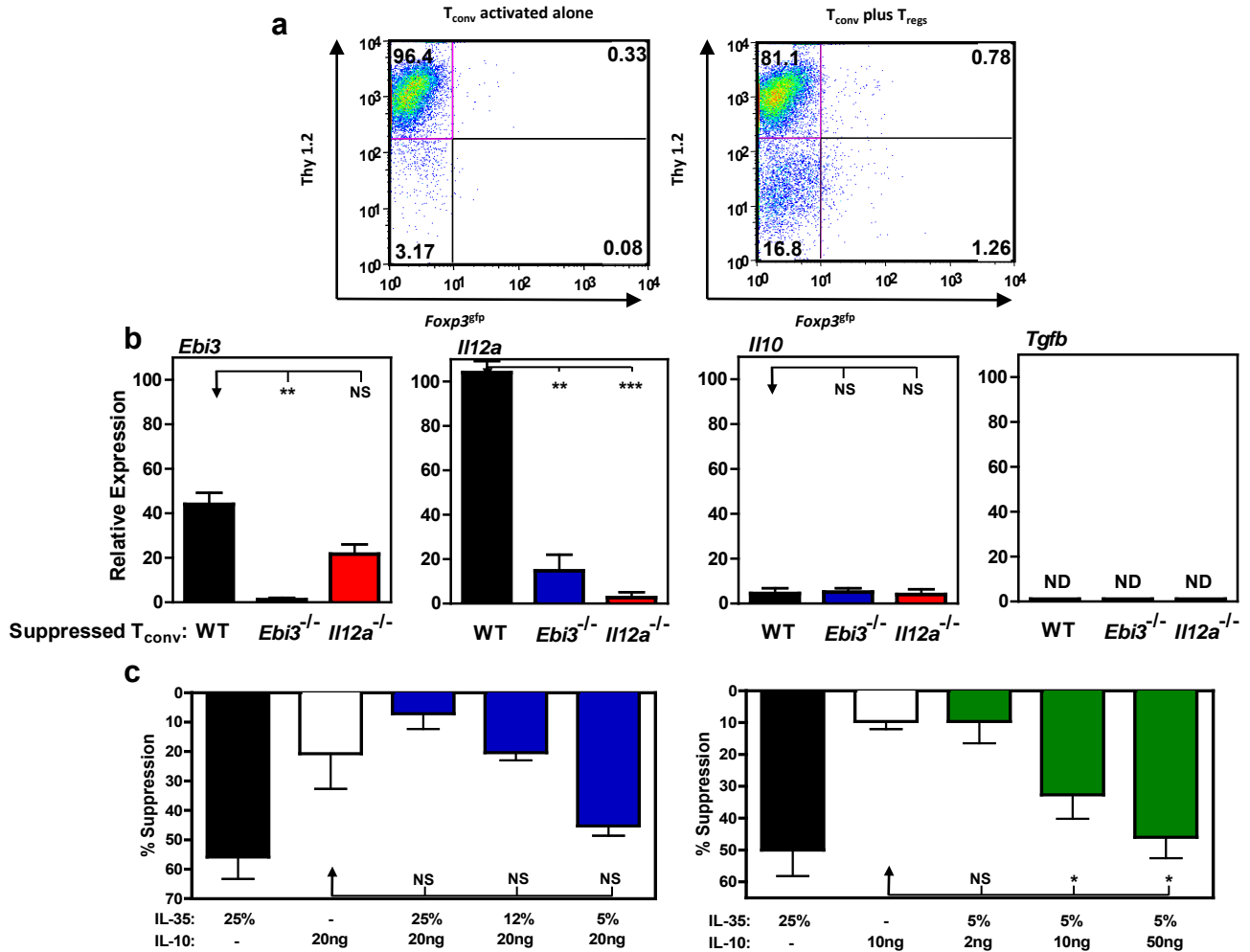
Supplementary Figure 14: TGFβ is not required for murine iT_{R35} mediated suppression *in vivo*. IBD was induced by injecting *Rag1*^{-/-} mice with wild type or TGFβRDN T_{conv} cells via the tail vein. After 3–4 weeks, mice developed clinical symptoms of IBD and were given iT_{R35} cells. (a) Percentage weight change after wild type or TGFβRDN T_{conv} cell transfer but before treatment with iT_{R35}. (b) Percentage weight change after iT_{R35} cell transfer. (c) Colonic histology scores of experimental mice. Crosses (†) indicate death of animals in groups not receiving iT_{R35}. Data represent 8–12 mice per group from 2 independent experiments. [NS = not significant]

Supplementary Figure 15



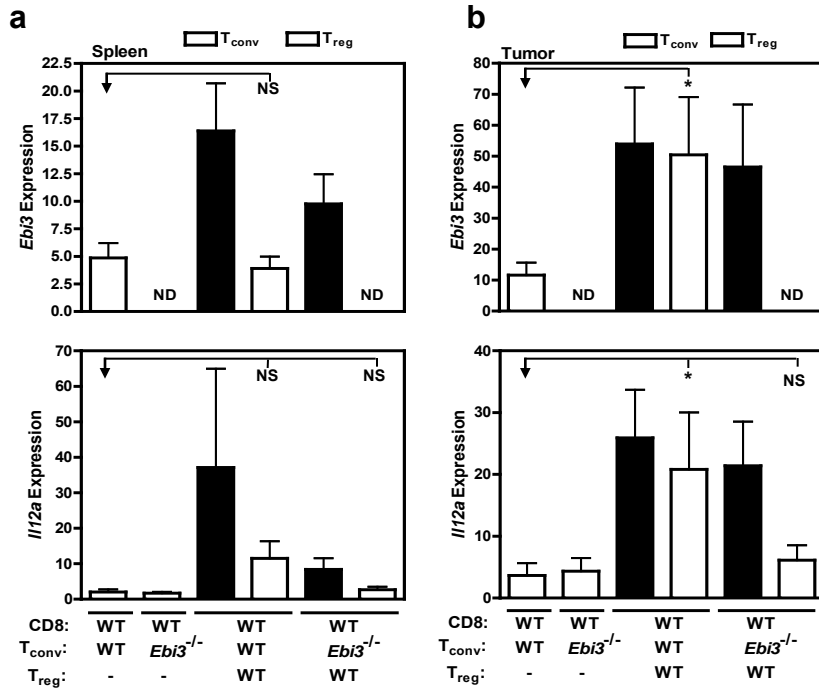
Supplementary Figure 15: Murine iT_{R35} stability *in vivo*. iT_{Rcontrol} or iT_{R35} were generated with CD45.2 murine T_{conv} cells and transferred into CD45.1 mice. At indicated times, CD45.2 cells were recovered from spleens of mice by FACS purification. (a–c) The suppressive capacity of iT_{Rcontrol} or iT_{R35} cells, compared to freshly sorted T_{regs} was determined by [³H]-thymidine incorporation. (d) From cells purified from stability experiments, RNA was isolated, cDNA generated and qPCR performed to verify expression of key molecules ascribed to each iT_R population, *Ebi3* and *Il12a* for iT_{R35} and *Foxp3* and *TGFβ* for TGFβ iT_R. For comparison, expression of *Ebi3*, *Il12a*, *Foxp3*, and *TGFβ* in freshly purified T_{conv} and T_{reg} is also included. Counts per minute of T_{conv} cells activated alone were 18,000–69,000 (a–c). Data represent the mean + SEM of 2–3 independent experiments, with at least 3 mice per experiment. [* p < 0.05, ** p < 0.005, NS = not significant]

Supplementary Figure 16



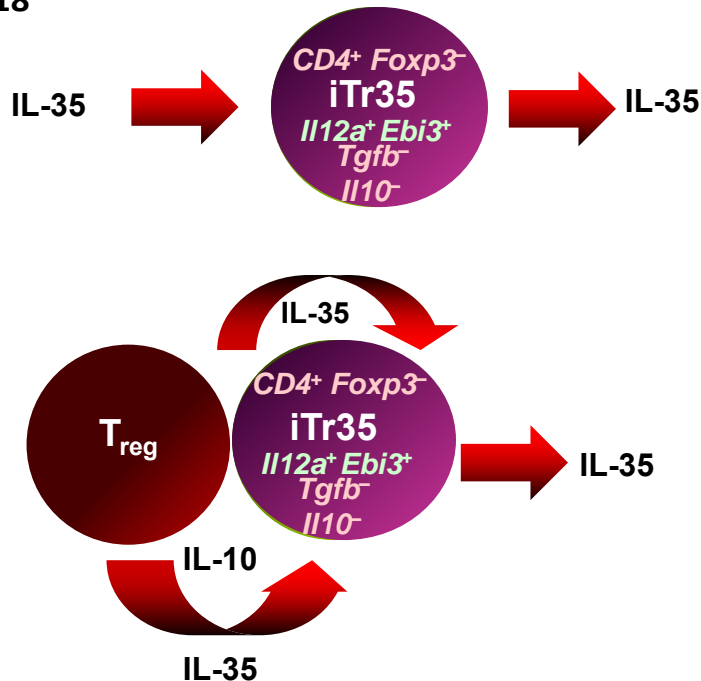
Supplementary Figure 16 : Phenotype and requirements for murine suppressed T_{conv} cell conversion and function. (a) T_{conv} from Thy 1.2 *Foxp3*^{9fp} mice were activated alone, or in the presence of Thy1.1 T_{reg} at a 4:1 ratio (responder: suppressor) for 72 h. Induction of Foxp3 expression was determined by flow cytometry. Data are representative of 2 independent experiments. (b) T_{conv} from wild-type C57BL/6, *Ebi3*^{-/-} or *Il12a*^{-/-} (p35) mice were activated in the presence of wild-type T_{reg} at a 4:1 ratio (responder: suppressor) for 72 h. Following co-culture, suppressed T_{conv} were re-purified, RNA was extracted and cDNA generated. Relative *Ebi3*, *Il12a*, *Il10* and *Tgfb* expression. Data represent the mean + s.e.m. of 4-6 independent experiments. (c). T_{conv} were activated in the presence of standard concentrations of IL-35 (25% of total volume) and IL-10 or suboptimal IL-35 and indicated concentrations of IL-10 for 72 h. Cells were purified following conversion and assayed for regulatory capacity towards fresh responder T_{conv} cells via [³H]-thymidine incorporation. Counts per minute of T_{conv} cells activated alone were 24,000-49,000 (c). Data represent the mean + SEM of 4-5 independent experiments. [* p < 0.05, ** p < 0.005, *** p < 0.001, NS not significant]

Supplementary Figure 17



Supplementary Figure 17: The suppressive T cell milieu in the tumor microenvironment is largely due to $i\text{T}_{R35}$. *Rag1*^{-/-} mice were reconstituted with wild type C57Bl/6 CD8⁺ T cells and wild type or *Ebi3*^{-/-} T_{conv} cells either with or without wild type T_{regs}. The following day, all mice were injected with 120,000 B16 cells i.d. on the right flank. Tumors and spleens were excised after 15-17 days and CD4⁺Foxp3⁻ and CD4⁺Foxp3⁺ cells were purified by FACS, RNA extracted and cDNA generated. (a) *Ebi3* (top panel) and *Il12a* (bottom panel) expression in the spleen (a) and tumor (b) Data represent the mean ± SEM of 8-10 mice per group from 3 independent experiments. [* p < 0.05, NS = not significant]

Supplementary Figure 18



Supplementary Figure 18: Model of $i\text{T}_{R35}$ Induction and Function.